High late Miocene–Pliocene elevation of the Zhada Basin, southwestern Tibetan Plateau, from carbonate clumped isotope thermometry

Katharine W. Huntington[1,†], Joel Saylor[2], Jay Quade[3], and Adam M. Hudson[3]
[1]*Department of Earth and Space Sciences, University of Washington, Seattle, Washington 98195, USA*
[2]*Department of Earth and Atmospheric Sciences, University of Houston, Houston, Texas 77204, USA*
[3]*Department of Geosciences, University of Arizona, Tucson, Arizona 85721, USA*

ABSTRACT

The timing and pattern of Tibetan Plateau rise provide a critical test of possible mechanisms for the development and support of high topography, yet views range widely on the history of surface uplift to modern elevations of ~4.5 km. To address this issue we present clumped isotope thermometry data from two well-studied basins in central and southwestern Tibet, for which previous carbonate $\delta^{18}O$ data have been used to reconstruct high paleoelevations from late Oligocene to Pliocene time. Clumped isotope thermometry uses measurements of the ^{13}C-^{18}O bond ordering in carbonates to constrain the temperature [$T(\Delta_{47})$] and $\delta^{18}O$ value of the water from which the carbonate grew. These data can be used to infer paleoelevation by exploiting the systematic decrease of surface temperature and the $\delta^{18}O$ value of meteoric water with elevation, provided samples record original depositional conditions and appropriate context exists for interpreting $T(\Delta_{47})$ and $\delta^{18}O$ values.

Previous calcite $\delta^{18}O$ and $\delta^{13}C$ values for Oligocene-age marls from the Nima Basin in central Tibet are thought to reflect original depositional conditions; however, $T(\Delta_{47})$ values exceed Earth-surface temperatures, indicating that the samples have been diagenetically altered. Maximum burial temperatures were not high enough to cause solid-state C-O bond reordering. Instead, the elevated $T(\Delta_{47})$ and water $\delta^{18}O$ values are consistent with recrystallization of the samples in a rock-buffered system.

Miocene–Pliocene aragonitic gastropod shells from the Zhada Basin in southwestern Tibet record primary environmental temperatures, which we interpret in the context of modern shell and tufa $T(\Delta_{47})$ values and lake water temperatures. Modern shell and tufa $T(\Delta_{47})$ values are similar to warm-season water temperatures. The ca. 9–4 Ma shell temperatures are significantly colder, suggesting a 9 ± 3 °C (2σ) average increase in warm-season lake water temperatures since the late Miocene. If the temperature increase is due entirely to elevation change and the modern June-July-August (JJA) surface water lapse rate of 6.1 °C/km applies, it implies >1 km of elevation loss since the late Miocene–Pliocene—corresponding to an average basin floor paleoelevation of 5.4 ± 0.5 km (2σ). A warmer mid-Pliocene climate would make this a minimum estimate. Our finding of cold paleotemperatures contrasts with previous conclusions based on Pliocene snail shell $T(\Delta_{47})$ data interpreted in the absence of modern shell and water temperature data, but is consistent with $\delta^{18}O$-based paleoaltimetry and with paleontological and isotopic data indicating the presence of cold-adapted mammals living in a cold, high-elevation climate. We suggest that late Neogene elevation loss across the Zhada Basin catchment probably related to local expression of east-west extension across much of the southern Tibetan Plateau at this time.

INTRODUCTION

Views range widely on the timing of surface uplift of the Tibetan Plateau to its current high (~4.5 km) elevation over a huge (>2.5 million km^2) area. Specifically, interpretations differ on whether the modern high elevations were recently developed or are largely a continuation of high elevations developed prior to Indo-Asian collision in the Eocene. For example, some workers suggest that Tibet rose comparatively recently, during the Neogene, either en masse (Molnar and Stock, 2009) or at least locally (Wang et al., 2006). Others propose that high elevations in at least southern Tibet were inherited from a high-standing, Paleogene or earlier pre-collision plateau informally referred to as the "Lhasaplano" (Kapp et al., 2007). The views of Rowley and Currie (2006) and Polissar et al. (2009) lie somewhere between these extremes, and begin with uplift of southern Tibet just after collision (Eocene), followed by the rise of the northern half of the plateau during the Miocene.

The timing and pattern of Tibetan Plateau uplift provide a critical test of these varying uplift scenarios and the possible underlying mechanisms. In this regard, stable isotopic evidence has assumed a key role in the reconstruction of paleoelevation not just in Tibet (e.g., Rowley et al., 2001; Rowley and Currie, 2006; Quade et al., 2011) but also in other orogens such as the Andes, Sierra Nevada, early Cenozoic Rockies, and Colorado Plateau (e.g., Garzione et al., 2008, 2014; Mulch et al., 2008; Cassel et al., 2009; Huntington et al., 2010; Lechler et al., 2013; Leier et al., 2013; Carrapa et al., 2014). This technique takes advantage of the sensitive relationship between the stable oxygen ($\delta^{18}O_{mw}$) and deuterium (δD_{mw}) composition of average meteoric water and elevation. Paleowater isotopic composition can be reconstructed from the isotopic compositions of geologic archives such as carbonates and waters of hydration in volcanic glass, provided that the relevant fractionation factors are known. For carbonates (but not volcanic glass), fractionation factors are temperature dependent, and therefore temperatures of carbonate formation must be assumed in order to reconstruct $\delta^{18}O_{mw}$.

Isotopic values of calcite, aragonite, and fossil bioapatite have provided the basis for most paleoelevation reconstructions in Tibet to date. For example, isotopic evidence suggests that high elevations were attained in southern Tibet by at least the Oligocene (Rowley and Currie, 2006; DeCelles et al., 2007b), and in northern Tibet much later, during the Mio-Pliocene (Cyr et al., 2005). However, reinterpretation of the northern Tibetan evidence based on modern patterns in $\delta^{18}O_{mw}$ points to attainment of high elevation well before the Miocene (Quade et al., 2011). Moreover, evidence from fossil tooth $\delta^{13}C$ values (Wang et al., 2006) challenges

†E-mail: kate1@uw.edu

GSA Bulletin; January/February 2015; v. 127; no. 1/2; p. 181–199; doi: 10.1130/B31000.1; 9 figures; 3 tables; Data Repository item 2014288; published online 7 August 2014.

the idea that even southern Tibet was elevated before the late Miocene.

In addition, the findings of Leier et al. (2009) on the susceptibility of carbonate $\delta^{18}O$ values to diagenetic resetting cast a long shadow over some of these studies. Leier et al. (2009) showed that mid-Cretaceous–age carbonates from Tibet, and early Miocene carbonates from Pakistan and Nepal, were isotopically reset during deep burial. Other studies present evidence that does redress aspects of the diagenesis issue (DeCelles et al., 2007b; Polissar et al., 2009; Snell et al., 2013), but our concerns remain that the $\delta^{18}O$ values of many basin carbonates in Tibet have been compromised by deep burial.

In this paper, we revisit with carbonate clumped isotope thermometry the conventional stable isotope studies of samples recording primary carbonate $\delta^{18}O$ values from two locations in Tibet, the Nima and Zhada Basins (DeCelles et al., 2007a, 2007b; Saylor et al., 2009) (Fig. 1). Clumped isotope thermometry is based on the temperature-dependent preference of ^{13}C and ^{18}O to form bonds with each other in the carbonate mineral lattice alone (measured using the parameter Δ_{47}), which constrains temperature without the need to assume the isotopic composition of the water from which the carbonate grew (Ghosh et al., 2006a; Eiler, 2007, 2011). Previous clumped isotope studies show that the method can be useful for paleoaltimetry (e.g., Ghosh et al., 2006b; Quade et al., 2007; Huntington et al., 2010; Leier et al., 2013; Lechler et al., 2013; Garzione et al., 2014), provided that the samples are well preserved and not reset by diagenesis, and that the paleotemperature calibrations based on modern samples are secure (e.g., Huntington et al., 2010). In this paper we both examine diagenetic resetting and report new data for modern samples to help interpret ancient sample data—from our own study and from four ca. 4 Ma samples from Zhada Basin (Wang et al., 2013)—using paleosol carbonate, aragonitic gastropods, and tufa from Tibet.

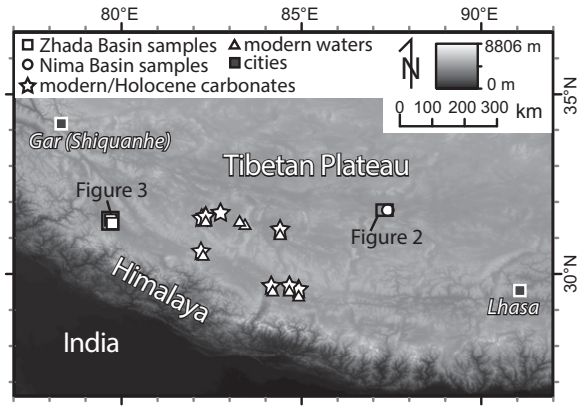

Figure 1. Digital elevation model of the southwestern Tibetan Plateau showing the locations of ancient basins and modern samples. Boxes outline the study areas in the Nima Basin (Fig. 2) and the Zhada Basin (Fig. 3).

GEOLOGIC SETTING AND PREVIOUS ISOTOPIC WORK

Our investigation focuses on fluvial-lacustrine carbonate deposits from the Nima and Zhada Basins, for which previous stable isotopic data have been used to reconstruct paleoelevation from late Oligocene to Pliocene time. Despite deep burial (~3 km) and elevated burial temperatures, previous work (DeCelles et al., 2007b) shows that Oligocene-age soil carbonate nodules from the Nima Basin yielded $\delta^{18}O$ and $\delta^{13}C$ values that very likely reflect original soil formation conditions at the surface. Much younger Miocene-age aragonite shell material from the Zhada Basin definitely preserves primary isotopic compositions (Saylor et al., 2009), reflecting formation in a range of aquatic environments. The Zhada and Nima samples make potentially very informative targets for clumped isotope analysis, providing tests of the effects of burial and potential diagenesis and of previous estimates of paleoelevation.

Nima Basin

In central Tibet, the Nima Basin (Fig. 2; ~32°N, ~87°E) currently sits at an elevation of 4.5–5 km in the Bangong suture zone separating the Qiantang and Lhasa terranes. The Nima Basin contains over 4 km of Tertiary basin fill including conglomerate, sandstone, marl, and paleosols (DeCelles et al., 2007a; Kapp et al., 2007). The Oligocene to mid-Miocene stratigraphy of the basin is dominated by the informally designated Nima Redbed unit, which comprises lacustrine marl beds and carbonate nodule–bearing paleosols constrained to be between 25 and 26 Ma in age based on dating of reworked tuff deposits within the unit (Kapp et al., 2007). The section sampled for stable isotope analysis, section 4DC in the Nima Redbed unit, was buried ~3 km, and possibly more depending on whether the nearby Nima fault once carried rocks in its hanging wall over the 4DC section (DeCelles et al., 2007a, 2007b).

Previous isotopic work in the Nima Redbed unit suggests that $\delta^{18}O$ and $\delta^{13}C$ values of lacustrine marl and paleosol calcite are primary (i.e., not diagenetically reset or reequilibrated during

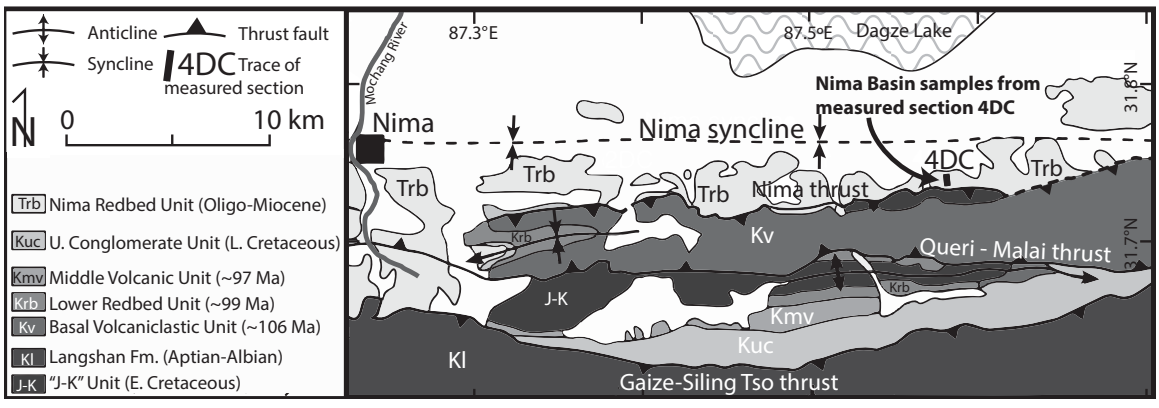

Figure 2. Geological map of the Nima area, modified from DeCelles et al. (2007a). Samples used in this study come from the "4DC" measured stratigraphic section (DeCelles et al., 2007b).

burial metamorphism) and indicate that the Nima Basin environment was arid and paleoelevation was ~4500–5000 m in the late Oligocene (DeCelles et al., 2007b). If the C and O bulk isotopic compositions of the calcites had been diagenetically altered since original deposition, homogenization of isotopes in initially heterogeneous phases of carbonate would be expected (Leier et al., 2009). DeCelles et al. (2007b) observed the opposite in a comparison of pedogenic carbonate and recycled marine limestone clasts deposited in the Nima Redbed unit: paleosol $\delta^{18}O$ and $\delta^{13}C$ values are tightly clustered and distinct from the wide range of isotopic values observed for recycled marine limestone clasts deposited throughout the same section, suggesting that the paleosol carbonates preserve original, unaltered $\delta^{18}O$ and $\delta^{13}C$ values (DeCelles et al., 2007b). Isotopic values for lacustrine marls in the same section are distinct from the paleosol values, with variable $\delta^{18}O$ values of –4.7‰ to –18.1‰ (Vienna Peedee belemnite, VPDB) reflecting varying degrees of evaporative ^{18}O enrichment in the lake waters from which the marls formed. Given that the $\delta^{18}O$ and $\delta^{13}C$ values of soil carbonate in the same section appear unaffected by burial diagenesis, it is reasonable to infer that the marls also record primary isotopic compositions consistent with a high, arid Nima Basin.

Taken together, the stratigraphy, structure, and isotopes from paleosols and marls from the Nima Basin paint a consistent picture of climate, topography, and elevation similar to today's since the late Oligocene (DeCelles et al., 2007a, 2007b; Kapp et al., 2007; Quade et al., 2011). While the quantitative paleoelevation estimate is based primarily on the $\delta^{18}O$ values of the least evaporatively enriched paleosol carbonates, the highly evaporatively enriched marl $\delta^{18}O$ values provide qualitative evidence that the climate was dry (DeCelles et al., 2007b). Although qualitative constraints on aridity from $\delta^{18}O$ values of lacustrine carbonates are useful, it is difficult to estimate either the lake water oxygen isotopic composition or temperature from these data alone.

Independent estimates of the temperature of carbonate formation from clumped isotope thermometry would enable estimates of both lake water temperature and $\delta^{18}O$ values, potentially placing more quantitative constraints on both lake hydrology (from paleowater $\delta^{18}O$ values) and paleoelevation. For instance, Huntington et al. (2010) showed that temperature estimates based on Δ_{47} values [$T(\Delta_{47})$] of modern lacustrine micrite and tufa from lakes in southwestern North America reflect warm-season temperatures, and decrease systematically with elevation, enabling them to estimate Colorado Plateau paleoelevation based on $T(\Delta_{47})$ values for Miocene lacustrine marls. A compilation and analysis of modern surface water temperature data from around the world (Hren and Sheldon, 2012) suggests that such an approach could be used to reconstruct paleoelevation from lacustrine carbonate temperatures in many environments—provided the temperatures they record are primary. Previous studies and age constraints make the Nima Basin marls attractive targets for clumped isotope paleoaltimetry. Moreover, the marls very probably retain primary $\delta^{18}O$ and $\delta^{13}C$ values from time of deposition even though they were deeply buried (~3 km) (DeCelles et al., 2007b), providing the opportunity to evaluate how well Δ_{47} values resist diagenetic resetting under these circumstances.

Zhada Basin

In southwestern Tibet, the late Cenozoic Zhada Basin (Fig. 3; ~31°N, ~80°E) sits at an elevation of 3.5–4.5 km and north of the Himalayan crest where it is bounded by the South Tibetan detachment system, Indus suture, and Leo Pargil and Gurla Mandhata gneiss domes. Incision by the Sutlej River has exposed the entire >800 m thickness of the Zhada Formation—an undisturbed sequence of fluvial, lacustrine, aeolian, and alluvial fan deposits (Saylor, 2008; Kempf et al., 2009; Saylor et al., 2009). The age of the Zhada Formation was constrained by magnetostratigraphy and biostratigraphic evidence to ca. 9.2 to <1 Ma (Zhang et al., 1981; Li and Li, 1990; Meng et al., 2008; Wang et al., 2008; Saylor et al., 2009).

Isotopic data from pristine aragonitic mollusk shells from the Zhada Basin and paleoenvironmental modeling point to a cold, arid Miocene–Pleistocene environment and suggest that the peaks surrounding the basin have been as high as or higher than the modern topography since at least 9 Ma (Saylor et al., 2009). Saylor et al. (2009) analyzed modern surface waters in the area and found that while river water $\delta^{18}O$ values are close to meteoric water values (or $\delta^{18}O_{mw}$), lake water $\delta^{18}O$ values are elevated due to evaporation. A similar pattern is apparent in the Miocene–Pliocene carbonates: $\delta^{18}O$ values of lacustrine mollusks are evaporatively enriched in ^{18}O, reflecting arid environmental conditions consistent with the occurrence of gypsum and mud cracks in the sediments, whereas $\delta^{18}O$ values of fluvial mollusks are much lower and provide the most accurate isotopic records of paleoelevation. Modern meteoric waters in the basin have extremely low $\delta^{18}O$ values due to the high elevations of the surrounding mountains (Garzione et al., 2000; Rowley et al., 2001); the lowest (least evaporative) estimates of Pleistocene–Miocene $\delta^{18}O_{mw}$ values, derived from lacustrine mollusk $\delta^{18}O$ values and the estimated temperature of carbonate formation, are even lower, indicating that the surrounding hydrologic basin was as least as high as and up to 1.5 km higher than today (Saylor et al., 2009).

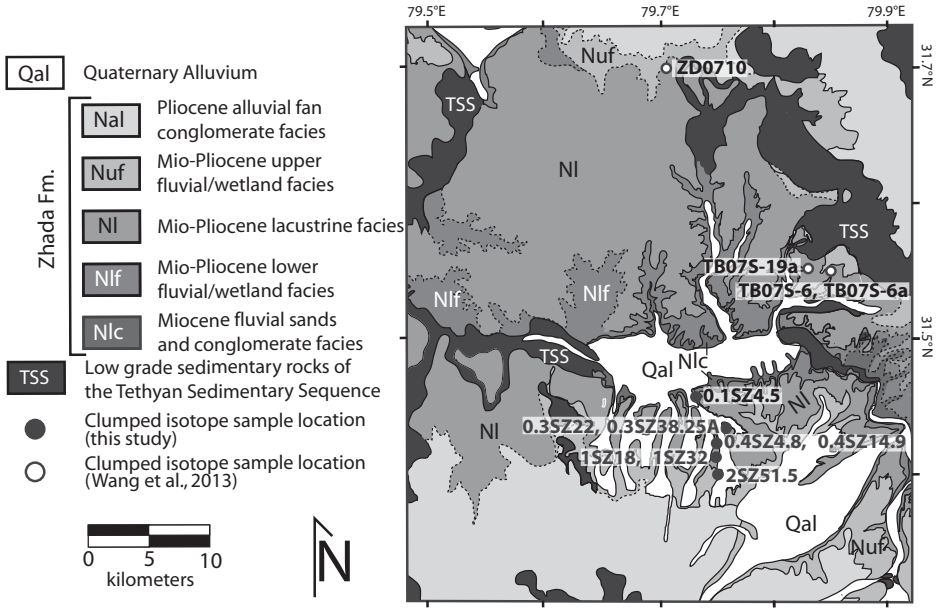

Figure 3. Geologic map of the central Zhada Basin, modified from Saylor et al. (2010), showing the location of samples used in this study and in Wang et al. (2013). Samples used in this study were analyzed by Saylor et al. (2009) and from the "South Zada" measured stratigraphic section of Saylor et al. (2010).

The need to assume the temperature of carbonate formation contributes to the uncertainty in $\delta^{18}O_{mw}$ values and in the resulting estimates of high paleoelevation and cold, arid conditions (Murphy et al., 2009; Saylor et al., 2009, 2010). Estimates of lake carbonate formation temperature typically are based on mean annual or growing-season air temperatures (Horton et al., 2004; Dettman et al., 2005; Saylor et al., 2009; Chamberlain et al., 2012). However, recent studies indicate that lacustrine carbonates reflect warm-season near-surface water temperatures (Huntington et al., 2010; Csank et al., 2011; Quade et al., 2011; Hren et al., 2013), which can be significantly different from either growing-season or mean annual air temperature (MAAT). Assuming little climate change between the Miocene and modern for the Zhada Basin, Saylor et al. (2009) estimated a shell aragonite formation temperature of 7 ± 7 °C above MAAT based on the average warm-season (April–October) air temperatures at a nearby weather station. However, Quade et al. (2011) studied lake carbonates (mid-Holocene tufa) on the Tibetan Plateau and inferred carbonate formation temperatures 12–23 °C above MAAT. If the offset between MAAT and Zhada Basin shell formation temperature is similar to the offset observed by Quade et al. (2011) for tufa formation, the temperature of shell precipitation would be at or above the high end of temperature estimated by Saylor et al. (2009). A warmer temperature estimate would increase reconstructed $\delta^{18}O_{mw}$ values and hence lower paleoelevations, raising the possibility that the high paleoelevation suggested by Saylor et al. (2009) is an artifact of their choice of temperature of shell precipitation.

Direct estimates of shell formation temperature from clumped isotopes both address this source of uncertainty in reconstructing $\delta^{18}O_{mw}$ values and provide independent constraints on elevation and environmental changes in the Zhada Basin. Deng et al. (2011, 2012) argued that the Zhada Basin was likely cooler during the late Miocene–early Pliocene based on the stable isotopic composition of fossil herbivores and occurrence in the basin of wooly rhinoceroses (*Coelodonta thibetana*) and three-toed horses (*Hipparion zandaense*) adapted to live in cold climates above the tree line. However, palynology and other mammal megafauna records from the Zhada Basin suggest a warmer and more humid late Miocene climate (Li and Li, 1990; Li and Zhou, 2001a, 2001b; Meng et al., 2004; Zhu et al., 2007). Clumped isotope paleotemperature estimates provide the means to evaluate these claims and estimates of $\delta^{18}O_{mw}$ derived from the Zhada Basin gastropod $\delta^{18}O$ record.

METHODS

Sample Selection and Preparation

We targeted samples previously analyzed by DeCelles et al. (2007b) and Saylor et al. (2009) for paleoaltimetry, including seven early Miocene marl samples from the southern part of the Nima Basin (Table 1) and eight Miocene to Pliocene gastropod samples from the Zhada Basin (Table 2). The Nima Basin marls are lacustrine in origin and consist of dense, well-indurated micrite, are massive to delicately laminated, and contain fossil gastropods, ostracodes, and *Chara* that appear petrologically and geochemically unaltered (DeCelles et al., 2007b). The marls are thought to represent carbonate deposition in evaporative lakes during highstands, consistent with the occurrence of mud cracks and evaporites within the section and evaporatively enriched carbonate $\delta^{18}O$ values (DeCelles et al., 2007a, 2007b). The structural position of the marl beds in the Nima syncline in the footwall of the Nima thrust (DeCelles et al., 2007a) suggests that the samples were buried to ~3 km depth. In the Zhada Basin, aquatic gastropods (extinct species *Veletinopsis spiralis* and *Radix zandaensis*; Han et al., 2012) were collected from the lower 400 m of the Zhada Formation (South Zhada measured section of Saylor et al., 2009) and reflect wetland interfluve, littoral lake-margin distributary channel, littoral delta front, and profundal lake environments. The gastropods were never deeply buried (<1 km), and they are all aragonitic, indicating excellent preservation of original biogenic carbonate (Saylor et al., 2009). We assign ages for gastropod samples based on the preferred magnetostratigraphic age correlation of Saylor et al. (2009).

We also collected a suite of modern/early Holocene samples including two Holocene tufa samples (calcite) from Ngangla Ring Tso ("Tso" is Tibetan for lake) in central Tibet, and eight shells of modern to Holocene aquatic gastropods (aragonite; *Radix* sp. and other lymnaeids; see Table 2) from the same lake system and from shallow wetlands in the region. The tufa samples (Table 2, Kailas 20-1 and 20-2) were collected from the paleoshorelines of Ngangla Ring Tso. Dating of these tufas shows they are early Holocene in age (Hudson and Quade, 2013). Modern and early Holocene shells were also obtained from the same lake (nrc10 samples) and from a variety of other localities in southern Tibet (Tables 2, 3). Modern shell sample 2507-06-5 was collected in July 2006 (i.e., just before the summer monsoon season) from a stranded shell bed at the margin of a distributary system in the delta at the eastern end of Kungyu Tso (4876 m).

In many cases, water samples were collected directly from the water in which the modern mollusks were found. Water sample 250706-4 was collected from the distributary channel associated with modern shell sample 2507-06-5. Water was also collected from a small, unnamed pond (Table 3, Zhongba 10-6c) and flowing creek (Tsangpo27 H_2O), and from three large lakes (Tso Nag: nrc10-108-1; Ngangla Ring Tso: nrc10-56; Rinqen Shub Tso: nrc10-3a). At each sample site 15 ml of unfiltered water was sealed with Teflon and electrician's tape into a centrifuge tube and refrigerated in the laboratory. Water temperatures in which modern mollusks lived were obtained in mid-June at the time the samples were collected using a handheld digital thermometer. Long-term water temperature measurements were obtained from shallow water (~30 cm depth) of the large lake Ngangla Ring Tso using a Hobo temperature logger.

Marl and tufa samples were drilled with a slow Dremel tool, or chips of the samples were broken off and crushed gently with an agate mortar and pestle, to produce ~25 mg carbonate per sample. Gastropod samples were broken into fragments and cleaned using the following procedure: samples were sonicated for 1 min then rinsed repeatedly, first in deionized water (3–5 times), then in methanol (3–5 times), then again in deionized water (3 times). The cleaned shell fragments were dried at room temperature in a desiccator and powdered gently with an agate mortar and pestle.

Isotopic Analysis

$\delta^{18}O$ and δD Measurements of Water Samples

Water sample $\delta^{18}O$ values were measured using the CO_2 equilibration method on an automated sample preparation device attached directly to a Finnigan Delta S mass spectrometer at the University of Arizona. The δD values of water were measured using an automated chromium reduction device (H-Device) attached to the same mass spectrometer. The values were corrected based on internal lab standards, which are calibrated to Vienna standard mean ocean water (VSMOW) and SLAP (standard light Antarctic precipitation). The analytical precision for $\delta^{18}O$ and δD measurements is 0.08‰ and 0.6‰, respectively (1σ). Water isotopic results are reported using standard δ–per mil notation relative to VSMOW (Table 3).

$\delta^{18}O$, $\delta^{13}C$, and Δ_{47} Measurements of Carbonate Samples

Isotopic analyses ($\delta^{18}O$, $\delta^{13}C$, and Δ_{47}, a measure of the ^{13}C-^{18}O bond ordering in the carbonate) were performed on ~8 mg aliquots of the carbonate samples at the California Institute of

TABLE 1. SUMMARY OF CLUMPED ISOTOPIC DATA FOR THE NIMA BASIN SAMPLES

Sample	Sample description	Analytical method	$\delta^{13}C$, measured* (‰)	$\delta^{18}O_{carb}$, measured* (‰)	Δ_{47} (Caltech) (‰)	±1 SE (‰, analytical)	Δ_{47} (ARF) (‰)	Sample average Δ_{47} (Caltech) (‰)	±1 SE (‰, external)	$T(\Delta_{47})$ (Caltech, Zaarur) (°C)	±1 SE (°C)	$\delta^{18}O_{H_2O}$, calculated† (Caltech, Zaarur) (‰ VSMOW)	±1 SE (‰)
4 DC 34	Layered marl	MS-I	–4.4	–13.8	0.621	0.009	0.67	0.624	0.006	30	2	–10.6	0.6
		MS-I	–4.9	–14.0	0.631	0.008	0.68						
		MS-I	–4.4	–13.8	0.620	0.008	0.67						
4 DC 47	Layered marl	MS-I	0.4	–9.2	0.522	0.007	0.57	0.522	0.010§	61	4	–0.3	0.8
4 DC 51	Layered marl	MS-II	–0.4	–16.2	0.578	0.010	0.63	0.565	0.013	47	4	–9.6	0.9
		MS-I	–0.5	–16.0	0.551	0.010	0.60						
4 DC 105	Layered marl	MS-II	0.2	–14.1	0.592	0.009	0.64	0.560	0.033	49	10	–7	2
		MS-I	0.0	–14.1	0.527	0.007	0.57						
4 DC 112	Layered marl	MS-II	–1.1	–12.7	0.623	0.008	0.67	0.569	0.054	46	15	–6	3
		MS-I	–1.1	–12.4	0.516	0.009	0.56						
Nema 6A	Marl	MS-II	–0.1	–13.1	0.571	0.010	0.62	0.571	0.010§	45	3	–7.0	0.7
Nema 10.1	Marl	MS-I	–0.4	–16.1	0.562	0.008	0.61	0.562	0.010§	48	3	–9.5	0.7

Note: See text for description of absolute reference frame (ARF) and California Institute of Technology (Caltech) reference frames. Fractionation factor for calcite from Kim and O'Neil (1997). Nima Basin marl samples (calcite) from section 4DC (DeCelles et al., 2007a): 31.7735°N, 87.5704°E, 4630 m elevation. SE—Standard error. MS-I and MS-II refer to the analytical methods associated with the two Caltech mass spectrometers (see text for details). Zaarur indicates that temperatures were calculated using the Zaarur et al. (2013) clumped isotope temperature calibration (see text for details).

*Measured versus Vienna Peedee belemnite (VPDB).

†Measured versus Vienna standard mean ocean water (VSMOW).

§Samples not externally replicated, so errors reflect actual analytical error for the sample, or long-term error in standard analyses, whichever is larger.

Technology (Caltech) using two Thermo MAT 253 mass spectrometers (MS-I and MS-II) configured to measure m/z 44–49 inclusive (Eiler and Schauble, 2004; Affek and Eiler, 2006). The MS-I samples were digested in phosphoric acid at 25 °C, and the product CO_2 was purified following the methods of Ghosh et al. (2006a) and Huntington et al. (2010). MS-II samples were digested at 90 °C, and the product CO_2 was purified following Passey et al. (2010). For samples digested at 90 °C, the reported Δ_{47} value includes an acid digestion correction of 0.081‰, which was determined empirically in the Caltech lab using the same methods and during the same time period over which the samples were analyzed (Passey et al., 2010). Analyses were screened for contaminants using mass-48 values (Eiler and Schauble, 2004; Guo and Eiler, 2007), and results are reported only for samples with Δ_{48} values within 2‰ of the heated gas δ_{48} versus Δ_{48} line (e.g., Huntington et al., 2009). The in-house carbonate Δ_{47} standard Carrara marble was analyzed along with the samples (accepted Δ_{47} value 0.352‰ in the Caltech reference frame—see below) and yielded an average value of 0.345 ± 0.010‰ for MS-I and 0.350 ± 0.009‰ for MS-II (1σ), demonstrating that discrepancies due to methodological differences in acid digestion temperature and mass spectrometry on the two Caltech instruments are generally similar to the reported analytical uncertainties (see the GSA Data Repository[1] for carbonate standard and heated gas data). No systematic offset in Δ_{47} values was observed among replicate analyses of different aliquots of the same samples measured on the two different mass spectrometers. The $\delta^{18}O$ and $\delta^{13}C$ values are referenced to VPDB.

The analyses were conducted prior to the creation of the absolute reference frame (carbon dioxide equilibrium scale) described by Dennis et al. (2011), so we report Δ_{47} data relative to the Caltech intralab reference frame (also known as "older " or "heated gas" reference frame) described by Huntington et al. (2009). In the Caltech reference frame, the data are normalized and corrected for scale compression using heated gases like the initial calibration data of Ghosh et al. (2006a). At this time some uncertainty exists regarding the consistency of calibrations across different laboratories; however, the discrepancies are on the order of the analytical uncertainties reported in this study, and it appears that they arise due to differences in the materials and methods of sample preparation

[1]GSA Data Repository item 2014288, Table DR1. Isotopic results for carbonate standards and heated gases analyzed together with clumped isotope samples, is available at http://www.geosociety.org/pubs/ft2014.htm or by request to editing@geosociety.org.

TABLE 2. SUMMARY OF CLUMPED ISOTOPIC DATA FOR THE ZHADA BASIN AND MODERN/HOLOCENE GASTROPOD AND TUFA SAMPLES

Sample	Sample description	Latitude (°N)	Longitude (°E)	Elevation (m)	Analytical method	$\delta^{13}C$, measured* (‰)	$\delta^{18}O_{carb}$, measured* (‰)	Δ_{47} (Caltech) (‰)	±1 SE (‰, analytical)	Δ_{47} (ARF) (‰)	Sample average Δ_{47} (Caltech) (‰)	±1 SE (‰, external)	$T(\Delta_{47})$ (Caltech, Eagle) (°C)	±1 SE (°C)	$\delta^{18}O_{H_2O}$, calculated† (Caltech, Eagle) (‰ VSMOW)	±1 SE (‰)	$T(\Delta_{47})$ (Caltech, Henkes) (°C)	±1 SE (°C)	$\delta^{18}O_{H_2O}$, calculated† (Caltech, Henkes) (‰ VSMOW)	±1 SE (‰)
South Zhada Basin, aragonitic gastropod samples, this study and Wang et al. (2013):																				
ZD0710	Age 3.7 Ma, Wang et al. (2013)	31.5	79.6	4210	MS-II	–0.1	–2.9	0.708	–	0.76	0.708	0.025	4	4	–6	1	–2	4	–7	1
TB07S-6	Age 4 Ma, Wang et al. (2013)	31.5	79.6	4190	MS-II	–0.7	–3.3	0.716	–	0.77	0.716	0.025	2	4	–7	1	–5	4	–8	1
TB07S-6a	Age 4 Ma, Wang et al. (2013)	31.5	79.6	4190	MS-II	–2.4	–3.9	0.700	–	0.75	0.700	0.025	6	4	–7	1	0	4	–8	1
2 SZ 51.5	Lake-plain supra-littoral, lake-margin distributary channel; 4.2 Ma#	31.40973	79.75618	4050	MS-II MS-I MS-I	–0.4 –0.4 –0.4	–2.4 –2.3 –2.3	0.694 0.665 0.659	0.009 0.009 0.009	0.75 0.72 0.71	0.673	0.011	14	3	–3.0	0.7	9	3	–4.1	0.8
TB07S-19a	Age 4.4 Ma, Wang et al. (2013)	31.5	79.6	4120	MS-II	–4.0	–4.0	0.685	–	0.74	0.685	0.025	11	4	–6	1	5	4	–7	1
1 SZ 32	Profundal claystone; 4.7 Ma#	31.42125	79.74981	4000	MS-II MS-I MS-I	1.5 1.5 1.5	–2.5 –2.3 –2.4	0.698 0.692 0.667	0.008 0.007 0.009	0.75 0.74 0.72	0.685	0.009	10	2	–3.9	0.5	5	2	–5.1	0.6
1 SZ 18	Littoral, lake margin, distributary; 4.9 Ma#	31.42125	79.74981	3980	MS-II MS-I	0.6 0.6	–3.8 –1.8	0.698 0.686	0.009 0.008	0.75 0.74	0.692	0.007§	9	2	–5	1	3	2	–6	1
0.4 SZ 14.9	Littoral, delta front, flooding; 5.1 Ma#	31.42512	79.75197	3950	MS-II MS-I	–7.3 –7.3	–18.7 –18.6	0.701 0.686	0.009 0.008	0.75 0.74	0.693	0.008	8	2	–20.7	0.5	2	2	–22.0	0.6
0.4 SZ 4.8	Littoral lake-margin distributary channel; 5.2 Ma#	31.42512	79.75197	3940	MS-II MS-I	–1.7 –1.9	–1.4 –1.3	0.680 0.683	0.009 0.009	0.73 0.74	0.682	0.007§	12	2	–2.4	0.5	6	2	–3.8	0.6
0.3 SZ 38.25A	Littoral lake-margin distributary channel; collected 16 m higher than 0.3 SZ 22; 5.5 Ma#	31.43766	79.75238	3910	MS-II MS-II MS-I MS-I	–1.8 –1.9 –1.9 –1.9	–6.9 –6.6 –6.8 –6.8	0.699 0.709 0.658 0.675	0.009 0.010 0.009 0.008	0.75 0.76 0.71 0.73	0.685	0.011	11	3	–8.1	0.8	5	3	–9.4	0.8
0.3 SZ 22	Littoral lake-margin distributary channel; 6.1 Ma#	31.43766	79.75238	3900	MS-II MS-II MS-I	–2.7 –2.4 –2.8	–8.3 –7.6 –8.2	0.661 0.677 0.667	0.010 0.015 0.010	0.71 0.73 0.72	0.669	0.006§	16	2	–8.3	0.8	11	2	–9.3	0.8
0.1 SZ 4.5	Floodplain wetland interfluve, stagnant to semi-stagnant; 8.5 Ma#	31.46810	79.72152	3750	MS-II MS-I MS-I	–1.1 –1.1 –1.1	–2.5 –2.0 –2.1	0.688 0.670 0.694	0.007 0.009 0.009	0.74 0.72 0.75	0.684	0.007	11	2	–3.5	0.7	5	2	–4.9	0.8

(*continued*)

TABLE 2. SUMMARY OF CLUMPED ISOTOPIC DATA FOR THE ZHADA BASIN AND MODERN/HOLOCENE GASTROPOD AND TUFA SAMPLES (*continued*)

Sample	Sample description	Latitude (°N)	Longitude (°E)	Elevation (m)	Analytical method	$\delta^{13}C$, measured* (‰)	$\delta^{18}O_{carb}$, measured* (‰)	Δ_{47} (Caltech) (‰)	±1 SE (‰, analytical)	Δ_{47} (ARF) (‰)	Sample average Δ_{47} (Caltech) (‰)	±1 SE (‰, external)	$T(\Delta_{47})$ (Caltech, Eagle) (°C)	±1 SE (°C)	$\delta^{18}O_{H_2O}$, calculated† (Caltech, Eagle) (‰ VSMOW)	±1 SE (‰)	$T(\Delta_{47})$ (Caltech, Henkes) (°C)	±1 SE (°C)	$\delta^{18}O_{H_2O}$, calculated† (Caltech, Henkes) (‰ VSMOW)	±1 SE (‰)
Modern/Holocene aragonitic gastropod samples:																				
nrc10-107-1	Lymnaeid, 9315 ± 170 ^{14}C yr, complete white shell, from shoreline, fractured aperture	31.58175	82.33985	4830	MS-II	–2.5	–9.1	0.679	0.014	0.73	0.679	0.014**	12	3	–10.2	0.9	7	3	–11.3	0.9
nrc10-114-4	Lymnaeid, Holocene, small complete white shell	31.54211	82.29422	4830	MS-II	–4.4	–12.1	0.660	0.011	0.71	0.660	0.011**	18	3	–11.9	0.8	14	3	–12.8	0.8
nrc10-108-2	Lymnaeid, modern, complete white shell	31.58836	82.33525	4810	MS-II	–2.6	–7.5	0.660	0.010	0.71	0.660	0.010**	18	2	–7.3	0.6	14	2	–8.2	0.6
2507-06-5	Stranded shell bed at margin of delta, east end of Kungyu Tso	30.64408	82.21315	4880	MS-I MS-I	–4.1 –4.2	–3.7 –3.8	0.692 0.687	0.009 0.008	0.74 0.74	0.689	0.007§	9	2	–5.5	0.6	4	2	–6.6	0.7
DT 10-9-3	*Radix* lymnaeid, modern, living in creek, complete white shell, fractured aperture	31.23498	84.39553	4550	MS-II	–9.1	–7.8	0.626	0.015	0.68	0.626	0.015**	30	4	–5	1	28	4	–5	1
Zhongba 10-7-2	Lymnaeid, *Gyraulus*, Holocene, fractured pieces of shell	29.6660	84.16774	4570	MS-II	–5.2	–15.3	0.664	0.011	0.72	0.664	0.011**	17	3	–5.3	0.8	13	3	–6.1	0.9
Zhongba 10-6b	Lymnaeid, *Gyraulus*, modern, fractured pieces of shell, small interdune pool	29.66627	84.66669	4570	MS-II	–7.6	–10.8	0.624	0.011	0.67	0.624	0.011**	31	3	–8.0	0.8	28	3	–8.6	0.8
Zhongba 10-10a	Lymnaeid, modern, living, complete brown shell	29.66738	84.1736	4570	MS-II	–5.8	–16.1	0.653	0.011	0.70	0.653	0.011**	21	3	–15.3	0.8	16	3	–16.4	0.8
Tsangpo 27	*Radix* lymnaeid, modern, living, from creek margin, fractured pieces of shell	29.55814	84.92331	4580	MS-II	–4.0	–17.7	0.658	0.010	0.71	0.658	0.010**	19	3	–17.3	0.8	15	3	–18.2	0.8

(*continued*)

TABLE 2. SUMMARY OF CLUMPED ISOTOPIC DATA FOR THE ZHADA BASIN AND MODERN/HOLOCENE GASTROPOD AND TUFA SAMPLES (*continued*)

Sample	Sample description	Latitude (°N)	Longitude (°E)	Elevation (m)	Analytical method	$\delta^{13}C$, measured* (‰)	$\delta^{18}O_{carb}$, measured* (‰)	Δ_{47} (Caltech) (‰)	±1 SE (‰, analytical)	Δ_{47} (ARF) (‰)	Sample average Δ_{47} (Caltech) (‰)	±1 SE (‰, external)	$T(\Delta_{47})$ (Caltech, Zaarur) (°C)	±1 SE (°C)	$\delta^{18}O_{H_2O}$, calculated† (Caltech, Zaarur) (‰ VSMOW)	±1 SE (‰)
Holocene tufa samples:																
Kailas 20-1	Holocene tufa (calcite), near Ngangla Ring Tso	31.6749	82.6988	4780	MS-II	2.1	–5.2	0.714	0.009	0.77	0.706	0.006§	10	2	–6.0	0.4
					MS-II	2.0	–5.2	0.706	0.009	0.76						
					MS-I	2.1	–5.1	0.700	0.009	0.75						
Kailas 20-2	Holocene tufa (calcite), near Ngangla Ring Tso	31.6749	82.6988	4820	MS-II	1.6	–5.8	0.714	0.010	0.77	0.686	0.015	15	3	–5.4	0.6
					MS-I	1.7	–5.6	0.663	0.011	0.71						
					MS-I	1.7	–5.6	0.682	0.009	0.73						

Note: See text for description of absolute reference frame (ARF) and California Institute of Technology (Caltech) reference frames, and for fractionation factors used for calcite and for aragonite. Uncertainty in sample elevations is ±10 m. "Eagle" refers to Eagle et al. (2013) aragonitic mollusk calibration, and "Henkes" refers to Henkes et al. (2013) mollusk and brachiopod calibration. MS-I and MS-II refer to the analytical methods associated with the two Caltech mass spectrometers (see text for details). Zaarur indicates that temperatures were calculated using the Zaarur et al. (2013) clumped isotope temperature calibration (see text for details).

*Measured versus Vienna Peedee belemnite (VPDB).

†Measured versus Vienna standard mean ocean water (VSMOW).

§Sample external reproducibility is fortuitously low, so we estimated external error using the long-term standard deviation of standards measured on this instrument during analytical session (0.01) divided by the square root of the number of analyses.

#Sample age based on magnetostratigraphic tie points of Saylor et al. (2009), with errors estimated to be ~100 k.y.

**Samples not externally replicated, so errors reflect actual analytical error for the sample, or long-term error in standard analyses, whichever is larger.

and acid digestion used in different laboratories. Thus for our sample data, we believe it is most appropriate to use calibrations generated using the same laboratory methods, with data referenced to the stochastic distribution. As a consequence, to convert sample Δ_{47} values into carbonate growth temperature estimates [$T(\Delta_{47})$], for calcite we use the Zaarur et al. (2011) synthetic carbonate calibration (Tables 1, 2). The Zaarur et al. (2011) calibration includes and is consistent with the original Ghosh et al. (2006a) calibration data that were generated in the same laboratory as our sample data, and sample temperatures calculated using the two calibrations are within error. For aragonitic gastropod shells we report temperatures calculated using both the Eagle et al. (2013) aragonitic mollusk and Henkes et al. (2013) mollusk/brachiopod calibrations referenced to the Caltech or "heated gas" reference frame (Table 2). We prefer the Eagle et al. (2013) calibration because the data were generated in the same laboratory as our sample data, the Henkes et al. (2013) calibration results in unrealistically low temperatures for some samples (Wang et al., 2013), and temperatures calculated with the Eagle et al. (2013) calibration generally result in closer correspondence between the measured and calculated $\delta^{18}O$ of water values for modern samples (Table 3). The sensitivity of our findings to the choice of calibration used to calculate temperature from the Δ_{47} values of aragonitic gastropod shells is explored below (see Discussion). Water $\delta^{18}O$ values were calculated from the sample $T(\Delta_{47})$ and $\delta^{18}O$ values using the fractionation factors of Kim and O'Neil (1997) and Kim et al. (2007) for calcite and aragonite, respectively.

ISOTOPIC RESULTS

Isotopic Results for Nima Basin Marl Samples

The Nima Basin $\delta^{13}C$ and $\delta^{18}O$ values (Table 1) are in excellent agreement with previously published isotopic values for the same samples reported by DeCelles et al. (2007b). The $\delta^{13}C$ values for individual analyses (–4.0‰ to 0.4‰ VPDB) are within 0.5‰ of published values. Similarly, $\delta^{18}O$ values for individual analyses from this study (–16.2‰ to –9.2‰ VPDB) are consistent with previously published $\delta^{18}O$ values for small samples of fresh micritic marl from throughout the section (–16.5‰ to –8.9‰), which were previously interpreted to reflect varying degrees of evaporative ^{18}O enrichment of lake waters in an arid environment (DeCelles et al., 2007b).

In contrast, most of the $T(\Delta_{47})$ estimates from these samples are well above Earth-surface

TABLE 3. ISOTOPIC COMPOSITIONS OF WATER COLLECTED WITH MODERN AND HOLOCENE GASTROPOD SHELL AND TUFA SAMPLES

Water sample	Latitude (°N)	Longitude (°E)	Elevation (m)	Water sample description	$\delta^{18}O_{H_2O}$, measured (‰ VSMOW)	Associated carbonate sample (living or non-living)	$\delta^{18}O_{carb}$, measured (‰ VPDB)	$\delta^{18}O_{carb}$, measured (‰, VSMOW)	$T(\Delta_{47})$ (°C)*	$\alpha^{\dagger}$	$\delta^{18}O_{H_2O}$, calculated (‰ VSMOW)	$\delta^{18}O_{H_2O}$, measured minus calculated (‰ VSMOW)
Modern waters from which modern gastropod shells were collected:						Modern samples:						
250706-4	30.64408	82.21315	4880	Kungyu Tso, inflow into lake	–15.6	2507-06-5, shell	–3.7	27.1	9	1.03276	–5.5	–10.1
nrc10-108-1	31.58836	82.33525	4800	Tso Nag, lake water	–5.4	nrc10-108-2, shell	–7.5	23.2	18	1.03073	–7.3	1.9
Zhongba 10-6c	29.66627	84.66669	4570	Small interdune pond water	–9.9	Zhongba 10-6b, shell	–10.8	19.8	31	1.02803	–8.0	–1.9
Tsangpo 27 H2O	29.55814	84.92331	4580	Margin of flowing creek water	–17	Tsangpo 27, shell	–17.7	12.7	19	1.03052	–17.3	0.3
DT 10-9-2	31.23498	84.39553	4550	Drebyur Tsaka, creek water	–10.1	DT 10-9-3, shell	–7.8	22.9	30	1.02823	–5.2	–4.9
Modern waters collected near Holocene shell and tufa sample locations:						Holocene samples:						
nrc10-3a	31.33015	83.42176	4770	Rinqen Shub Tso, lake water	–5.6	Kailas 20-1, tufa	–5.2	25.5	10	1.03175	–6.0	0.4
						Kailas 20-2, tufa	–5.6	25.1	15	1.03061	–5.3	–0.3
						nrc10-107-1, shell	–9.1	21.5	12	1.03207	–10.2	4.6
						nrc10-114-4, shell	–12.1	18.4	18	1.03073	–11.9	6.3
nrc10-56	31.47303	83.32535	4730	Ngangla Ring Tso, lake water	–3.7	Kailas 20-1, tufa	–5.2	25.5	10	1.03175	–6.0	2.3
						Kailas 20-2, tufa	–5.6	25.1	15	1.03061	–5.3	1.6
						nrc10-107-1, shell	–9.1	21.5	12	1.03207	–10.2	6.5
						nrc10-114-4, shell	–12.1	18.4	18	1.03073	–11.9	8.2

Note: VSMOW—Vienna standard mean ocean water; VPDB—Vienna Peedee belemnite.

*$T(\Delta_{47})$ values calculated using the aragonitic mollusk equation of Eagle et al. (2013) for aragonite, and non-biogenic equation of Zaarur et al. (2013) for calcite tufa.

†α value calculated using the equation of Kim et al. (2007) for aragonitic gastropod shell samples, or using the equation of Kim and O'Neil (1997) for calcite (tufa) samples.

temperatures, suggesting some degree of diagenetic resetting (Table 1). The warmest sample records an apparent temperature of 61 ± 4 °C (one standard error, SE), and the bulk $\delta^{13}C$ and $\delta^{18}O$ values are the most positive of the sample suite (0.4‰ and –9.2‰ VPDB, respectively). Five of the samples record $T(\Delta_{47})$ values within error of ~47 °C, and the similarity of isotopic values among these samples ($\delta^{13}C$ values of –1.1‰ to 0.2‰, and $\delta^{18}O$ values of –16.2‰ to –12.4‰ VPDB) suggests a shared diagenetic history. The final Nima Basin sample (4DC 34) records a much cooler temperature of 30 ± 2 °C (1 SE; 3 replicates), which is suspect given the obvious clumped isotope reordering in the other samples. Although this sample's $\delta^{18}O$ value is in line with the $\delta^{18}O$ values of the ~45 °C samples, its $\delta^{13}C$ value (–4.6‰ VPDB) is significantly lower. Regardless of whether or not the bulk $\delta^{13}C$ and $\delta^{18}O$ values of the Nima Basin samples are primary, high $T(\Delta_{47})$ values demonstrate that diagenesis (i.e., dissolution-reprecipitation or solid-state C-O bond reordering) has affected the samples in this section—preventing the $\delta^{18}O$ of water values calculated from the $T(\Delta_{47})$ and $\delta^{18}O$ of carbonate data shown in Table 1 from being used to estimate paleoelevation.

Isotopic Results for Zhada Basin Gastropod Samples

The $\delta^{13}C$ and $\delta^{18}O$ values of the Zhada Basin gastropod samples are within the range of values previously reported by Saylor et al. (2009) for other aragonitic gastropods from the section (Table 2). The $\delta^{13}C$ values from this study span a smaller range (–7.3‰ to 1.5‰ VPDB) than the previously published $\delta^{13}C$ values (–13.8‰ to 7.5‰ VPDB; Saylor et al., 2009), whereas the $\delta^{18}O$ values from this study (–18.7‰ to –1.3‰ VPDB) are in agreement with the large range of $\delta^{18}O$ values reported by Saylor et al. (2009).

The Zhada Basin $T(\Delta_{47})$ values are within the range of plausible Earth-surface temperatures (Table 2), consistent with the shallow burial and primary aragonitic composition of the samples. New $T(\Delta_{47})$ values for 8.5–4.2 Ma gastropods from this study range from 8 ± 2 °C to 16 ± 2 °C (1 SE), with an average temperature of 11 ± 3 °C (1σ; n = 8; Eagle et al. [2013] calibration). For comparison, Table 2 also shows the four previous analyses of 4.4–3.7 Ma gastropods from Wang et al. (2013), with temperatures recalculated using the Eagle et al. (2013) calibration. Temperature estimates for the 4.4 Ma Wang et al. (2013) sample (TB07S-19a, 11 ± 4 °C) and the 4.7 and 4.2 Ma samples from this study (10–14 °C) agree; however, the remaining three samples of Wang et al. (2013), which range in age from 3.7 to 4 Ma, yield temperature estimates of 2–6 °C that are colder than any of the other modern or late Miocene–Pliocene Zhada Basin samples. The temperature difference could be real; however, due to differences in analytical procedures, the Wang et al. (2013) samples may not be directly comparable to the samples from this study and from the Eagle et al. (2013) calibration, which were analyzed at Caltech.

Combining our new temperature estimates with $\delta^{18}O$ values of the same samples yields calculated values of $\delta^{18}O_{mw}$ that range widely from –20.7‰ ± 0.5‰ to –2.4‰ ± 0.5‰ VSMOW, compared to values of –6‰ to –7‰ for the Wang et al. (2013) samples. The lowest $\delta^{18}O_{mw}$ value (–20.7‰) is for a sample from a littoral delta-front environment that would have experienced flooding, whereas samples with higher calculated $\delta^{18}O_{mw}$ values record conditions in a stagnant to semi-stagnant wetland interfluve and littoral to supralittoral lake margin distributary channels; this suggests that the isotopic variation may be attributed to the amount of evaporative ^{18}O enrichment in waters in different depositional environments. For reference, $T(\Delta_{47})$ and $\delta^{18}O_{mw}$ values calculated using the calibration of Henkes et al. (2013) are also reported in Table 2.

Isotopic Results for Holocene to Modern Tufa, Gastropod, and Water Samples

We report results for 11 Holocene–modern carbonates (Table 2) in order to provide context for interpreting the Zhada Basin aragonite $T(\Delta_{47})$ records. The Holocene samples span an array of aquatic environments, much like the Zhada carbonates, from lakes to marshes to a flowing river. Isotopic results for the two lacustrine tufa samples from Ngangla Ring Tso are similar, with $\delta^{13}C$ and $\delta^{18}O$ values around –2‰ and –5‰ VPDB, respectively. We monitored

the shore-zone water temperature of a modern lake remnant (Ngangla Ring Tso) of the paleolake with which the early Holocene tufa samples are associated. We recorded summer average to maximum temperatures in the 13–17 °C range (Fig. 4), which overlaps the clumped isotope paleotemperatures from the tufa of 10–15 °C. Calculated $\delta^{18}O$ values of the waters from which the two tufa samples precipitated are –6.0‰ and –5.4‰ VSMOW. These values are close to $\delta^{18}O_{mw}$ values between –3.7‰ and –5.6‰ VSMOW of two large remnant lakes (Rinqen Shub Tso and Ngangla Ring Tso) of this system today (Table 3). Together, these data suggest that tufa is forming at or near isotopic equilibrium for both clumped isotopes, as calculated from Zaarur et al. (2011), and for $\delta^{18}O$ values, as calculated from Kim and O'Neil (1997).

The isotopic values for the ten modern and Holocene shells (aragonite) were more variable, with $\delta^{13}C$ values ranging from –2.5‰ to –9.1‰ and $\delta^{18}O$ values ranging from –3.7‰ to –17.7‰ VPDB. In contrast, $T(\Delta_{47})$ values on nearby samples agree, with one exception. The nrc10 samples (one modern, two Holocene) were collected within 7 km of each other at elevations of 4810–4830 m. Their $\delta^{13}C$ values vary by 2‰ and $\delta^{18}O$ values vary by nearly 5‰, whereas their $T(\Delta_{47})$ values are indistinguishable (18 ± 2 °C, 18 ± 3 °C, 12 ± 3 °C). Zhongba 10-7-2 (Holocene), 10-6b (modern), and 10-10a (modern) were collected from small interdune ponds within 1 km of each other at ~4570 m. Two of the samples (10-7-2 and 10-10a) have indistinguishable $T(\Delta_{47})$ values. In contrast, Zhongba 10-6b yields a warmer temperature of 31 °C. One potential reason for the difference in temperature is variability in the connectivity of interdune ponds to the local groundwater table. The local environment of a shallow interdune pond that is isolated from local groundwater may be warmer than representative large lake or river water temperatures at the same elevation, whereas ponds that exchange with local groundwater would be buffered against warmer temperatures. Hudson et al. (2014) assessed the connectivity of the ponds to groundwater by ^{14}C dating modern samples; Zhongba 10-10a yielded an apparent >1000 yr age, indicating that the pond from which it was collected may exchange water with the local groundwater table, which would impart ^{14}C depleted carbon and buffer toward lower summer temperatures. In contrast, Zhongba 10-6b yielded ^{14}C values in equilibrium with the modern atmosphere, indicating that the pond from which it was collected was isolated from groundwater (Hudson et al., 2014), potentially resulting in higher temperatures than ponds buffered by groundwater exchange. Although we did not date Zhongba 10-7-2, its relatively low clumped isotope temperature suggests the waters from which it was collected may have been connected to groundwater. Tsangpo 27 (modern) was collected at similar elevations within 50–75 km of the three Zhongba sites. Tsangpo 27 yields a $T(\Delta_{47})$ value of 19 ± 3 °C, in agreement with the other modern gastropods collected from lakes and rivers at similar elevations. Sample DT10-9-3 was collected ~175 km north of these samples at 4545 m elevation and also yields a warm $T(\Delta_{47})$ value of 30 ± 4 °C, discussed below. The $\delta^{18}O_{mw}$ values calculated from these data are –5.3‰ to –11.9‰ VSMOW for the Holocene samples, and range from –5‰ to –17.3‰ VSMOW for the modern samples.

To evaluate the modern mollusk data, we compared measured $\delta^{18}O$ values of the five water samples with estimates of the $\delta^{18}O$ values of waters calculated from shell aragonite $T(\Delta_{47})$ and $\delta^{18}O$ values (Table 3). For three of the five modern gastropod shell-water sample pairs, the observed and calculated $\delta^{18}O$ of water values are within 2‰ of each other—on the order of the annual variation in water O-isotopic values observed in Tibetan lakes by Taft et al. (2013). Observed and calculated $\delta^{18}O$ of water values for the modern (living) gastropod-water sample pair from Drebyur Tsaka creek (DT 10-9-2 and 10-9-3) differed by 4.9‰ (Table 3). To bring the observed and calculated values within 2‰ of each other, the shell formation temperature would have to be 16 °C, similar to the other modern sample temperatures but considerably cooler than the apparent clumped isotope temperature of 30 °C. The warm apparent clumped isotope temperature is insensitive to the choice of calibration: both the Eagle et al. (2013) and Henkes et al. (2013) calibrations yield temperatures of 28–30 °C for this sample (Table 2), as does the inorganic carbonate calibration of Zaarur et al. (2011). Given the discrepancy between the measured and calculated $\delta^{18}O$ of water values and the inconsistency of the 30 °C temperature with the rest of the lake and creek water samples, we consider sample DT 10-9-2 to be unreliable and exclude it from further discussion. The largest discrepancy between measured and calculated $\delta^{18}O$ values of water is for fossil shell sample 2507-06-5, which was collected from a natural cut-bank exposure cut by a creek that feeds Kungyu Tso. The shell sample was collected on the assumption that the shell was formed in the ancestral creek, but the results and setting are more consistent with formation in paleolake Kungyu Tso. This would account for the mismatch between $\delta^{18}O$ values of the associated water (sample 250706-4) from the distributary of –15.6‰, and the predicted $\delta^{18}O$ water value of –5.5‰ based on the shell $T(\Delta_{47})$. The shell formation temperature would have to be impossibly low (~–23 °C) to reconcile the observed and calculated values, but the calculated shell $\delta^{18}O$ of water value is consistent with isotopic compositions of Tibetan closed-basin lakes reported here and elsewhere (Quade et al., 2011). Thus we suggest that the predicted and measured $\delta^{18}O$ of water values are different because the gastropod lived during a previous lake highstand rather than in the fluvial distributary setting where it was collected. Kungyu Tso occupies a closed basin that likely experienced major changes in depth in the past due to climate changes (Hudson and Quade, 2013).

We also compared $\delta^{18}O$ values of water from two modern lakes to values predicted by four Holocene tufa and gastropod shell samples collected nearby (Table 3). The two tufa samples predict water $\delta^{18}O$ values that are in excellent agreement with the modern lake water value from Rinqen Shub Tso, and within ~2‰ of the lake water value from Ngangla Ring Tso. The $\delta^{18}O$ values of water predicted by the Holo-

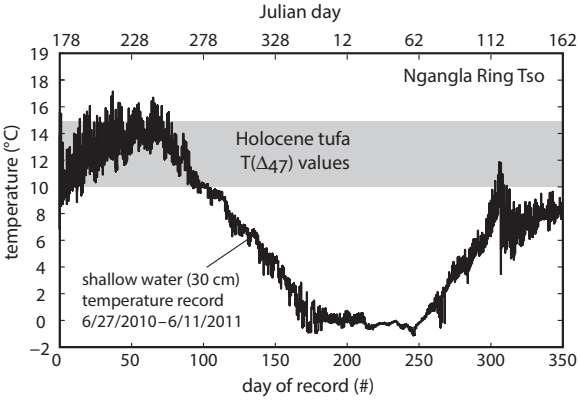

Figure 4. Surface water temperature monitoring data from Ngangla Ring Tso (lake). Long-term water temperature measurements were obtained from shallow water (at ~30 cm depth) along the lake margin using a Hobo temperature logger, which collected hourly temperature data between 27 June 2010 and 11 June 2011. Summertime lake surface water temperatures agree with formation temperatures [$T(\Delta_{47})$ values] of Holocene tufa samples collected from the lake's paleoshoreline.

cene shell samples differ from the modern Rinqen Shub Tso and Ngangla Ring Tso values by ~4‰–8‰.

DISCUSSION

We find that Miocene–Pleistocene aragonitic gastropods from the Zhada Basin record primary environmental temperatures that can potentially be used for paleoenvironmental reconstructions in the context of the observed $T(\Delta_{47})$ values of modern/Holocene gastropods from high elevation in Tibet. In contrast, and probably owing to deeper burial depths, the Δ_{47} values of marl samples from the Nima Basin have been reset to temperatures higher than typical of primary surface conditions.

Preservation of Isotopic Signals During Burial Reheating in the Nima Basin

We expected the Nima Basin sample $T(\Delta_{47})$ values to provide new paleoelevation constraints, but find temperatures that are above Earth-surface temperatures—indicating that the samples have experienced some degree of diagenetic alteration. When a carbonate mineral forms at Earth-surface temperatures, the ^{13}C-^{18}O bond ordering (i.e., the abundance of ^{13}C-^{18}O bonds in excess of the amount expected for a random distribution of isotopologues; Eiler, 2007) reflects the mineral growth temperature (e.g., Ghosh et al., 2006a; Schauble et al., 2006). However, during heating, this bond ordering is susceptible to resetting by diffusion of C and O through the solid mineral lattice (Dennis and Schrag, 2010; Passey and Henkes, 2012). Alternatively, clumped isotope bond ordering can be "reset" during burial if the samples are altered by mineral recrystallization (e.g., Schmid and Bernasconi, 2010; Huntington et al., 2011).

Cryptic recrystallization and/or diffusive C-O bond reordering within the Nima Basin samples may have been possible in light of the elevated temperatures experienced by the sampled section during burial, even though the samples are not obviously recrystallized and the calcite $\delta^{18}O$ and $\delta^{13}C$ values appear to be primary (DeCelles et al., 2007a, 2007b). For a nominal geothermal gradient of 25–30 °C/km, the samples' estimated burial depth of ~3 km (DeCelles et al., 2007b) corresponds to burial temperatures of around 75–90 °C. Whatever mechanism was responsible for the alteration of these samples must therefore be compatible with this burial history and explain the apparently primary calcite $\delta^{18}O$ and $\delta^{13}C$ values (DeCelles et al., 2007a, 2007b) and elevated clumped isotope temperatures of the samples.

We first evaluate the possibility that the elevated $T(\Delta_{47})$ values were caused by partial diffusive C-O bond reordering. Recent experiments indicate that a sample's thermal history and susceptibility to reordering dictate if and how much resetting occurs (Passey and Henkes, 2012). Case studies of natural marbles and carbonitites show that C-O bond reordering can occur at temperatures <200 °C (Dennis and Schrag, 2010), and indeed some paleosol carbonate samples of Quade et al. (2013) ceased to record primary surficial temperatures at maximum burial temperatures as low as ~80–90 °C. This is on the order of the temperatures likely experienced by the Nima Basin samples. However, Quade et al. (2013) left open the issue of whether their samples were altered by solid-state reordering or by micro-scale recrystallization that did not alter the micritic fabric of the samples. The most recent experimental data show that C-O reordering is negligible at temperatures below ~100 °C for timescales of ~1 m.y. and longer (Henkes et al., 2014). This indicates that the Nima Basin samples should not have been affected by diffusive C-O reordering if our estimate is correct and the burial temperature did not exceed ~75–90 °C.

A kinetic model of C-O bond reordering indicates that maximum burial temperatures would need to have been twice as hot for reordering to have caused the elevated $T(\Delta_{47})$ values. We used the model of Henkes et al. (2014) to explore temperature-time paths that could have initiated C-O bond reordering in the samples, varying (1) the maximum burial temperature (T_{max}) following deposition at 26 Ma and (2) the length of time the samples resided at T_{max} prior to cooling. If the samples resided at T_{max} only briefly (e.g., warm at constant rate from 26 to 13 Ma, reside at T_{max} for 0.5 m.y., and cool at constant rate to reach surface temperatures by 0 Ma), burial temperatures in excess of 160 °C would have been needed to cause resetting of the $T(\Delta_{47})$ values by C-O bond reordering (using Arrhenius parameters for brachiopod calcite; Henkes et al., 2014). This estimate is insensitive to the time at which T_{max} is reached. A slightly higher temperature of ~172 °C is required to produce the observed $T(\Delta_{47})$ values if Arrhenius parameters for optical calcite (Passey and Henkes, 2012) are used. A long (15 m.y.) residence time at T_{max} could produce the observed clumped isotope values with slightly lower maximum burial temperatures of 145–155 °C. The total measurable overburden is on the order of 3 km or less based on the maximum thickness of younger strata in the area, suggesting that the Nima samples were not significantly heated or more deeply buried. A doubling of the geothermal gradient or a doubling of the maximum burial estimate would be required to produce the Δ_{47} observations—strong evidence that diffusive C-O bond ordering did not affect the Nima Basin samples.

Instead, the data suggest that the elevated temperatures and apparently pristine carbonate $\delta^{18}O$ and $\delta^{13}C$ values resulted from varying degrees of micro-scale mineral recrystallization in a rock-buffered environment. Care was taken to sample only pristine-looking micritic carbonate (DeCelles et al., 2007b), but micro-scale solution-precipitation of calcite does not necessarily result in a loss of micritic texture and thus cannot be ruled out on this basis. In future studies, electron backscatter diffraction could be used to identify micro-scale recrystallization (e.g., Cusack et al., 2008; Pérez-Huerta et al., 2014). If recrystallization in a rock-buffered environment did occur, under warmer burial conditions the carbonate O-isotopic composition should remain approximately constant while the water O-isotopic values become enriched in ^{18}O and $T(\Delta_{47})$ increases (e.g., Henkes et al., 2014). To see if the data fit this hypothesized trend, we plotted $T(\Delta_{47})$ from Nima Basin carbonates versus the calculated $\delta^{18}O$ values of the waters from which the samples grew (Fig. 5). The coolest (30 °C) sample plots on the –14‰ (VPDB) carbonate $\delta^{18}O$ contour. The 45–49 °C samples plot within 2‰ of the –14‰ (VPDB) contour, in general agreement with the expected trend. The 61 °C sample plots on the –9‰ (VPDB) contour, suggesting growth at higher temperature from waters even more enriched in ^{18}O. The error bars are large, but the data are compatible with the hypothesis that the elevated clumped isotope temperatures were caused by micro-scale dissolution-reprecipitation. In this case, five of the samples must have cryptically recrystallized to similar degrees to yield very similar clumped isotope temperatures. We suggest that this is possible given the samples' similar textures and proximity to one another within 100 m in the same section.

Relationship Between Environmental Temperatures and $T(\Delta_{47})$ Values of Modern and Holocene Samples from Southeastern Tibet

Holocene tufa samples yielded $T(\Delta_{47})$ values that are consistent with one another and similar to modern summer surface lake water temperatures in the two large remnant lakes associated with these samples (Ngangla Ring Tso and Rinqen Shub Tso; Fig. 4). These data are consistent with the hypothesis that shallow lake carbonates form in the warm part of the year as previously suggested by Huntington et al. (2010) and Quade et al. (2011). Semiarid lake surface water temperatures and lacustrine carbonate Δ_{47}

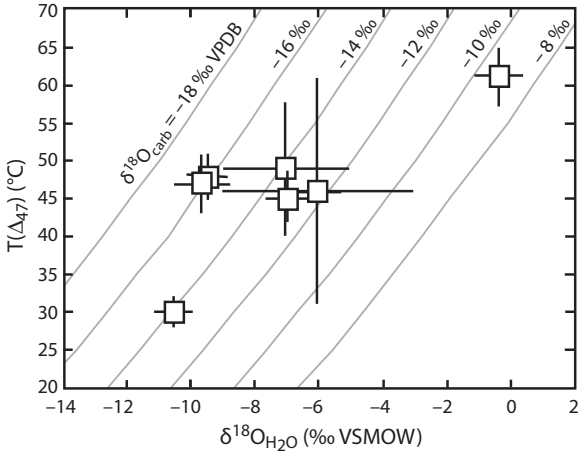

Figure 5. Nima Basin calcite clumped isotope temperatures [$T(\Delta_{47})$] versus apparent water oxygen isotope compositions of the waters from which the samples grew ($\delta^{18}O_{H_2O}$). Sample $T(\Delta_{47})$ values were calculated using the calibration of Eagle et al. (2013), and $\delta^{18}O_{H_2O}$ values were calculated using the calcite-water oxygen isotope thermometry equation of Kim and O'Neil (1997), as in Table 1. Squares are sample data with error bars indicating one standard error. Grey contours are solutions to the calcite-water oxygen isotope thermometry equations for constant $\delta^{18}O_{carb}$ values. If closed-system reordering is responsible for the elevated clumped isotope temperatures, $T(\Delta_{47})$ is expected to increase along contours of constant $\delta^{18}O_{carb}$. VSMOW—Vienna standard mean ocean water; VPDB—Vienna Peedee belemnite.

formation temperatures in the western United States suggest that $T(\Delta_{47})$ values for lakes above ~3500 m elevation may closely approximate average to maximum summer lake water temperatures (Huntington et al., 2010), consistent with our findings for these high-elevation Tibetan tufa samples. Calculated $\delta^{18}O$ values of the waters from which the tufa samples precipitated compare very closely to measured $\delta^{18}O_{mw}$ values of the modern remnant lakes of this system today (Table 3). Thus the tufa clumped isotope data are similar to modern summer water temperatures and modern lake $\delta^{18}O_{mw}$ values.

For the other modern sample locations, we calculated representative summer lake water temperatures using published relationships between elevation and mean annual air temperature (MAAT) and between MAAT and lake water temperature, using our instrumental record from Ngangla Ring Tso to test the fidelity of the approach. At Ngangla Ring Tso (elevation 4727 m), using the temperature-elevation equation of Quade et al. (2011) for the region (i.e., MAAT [°C] = –0.0081 × elevation [m] + 35.326; Fig. 6), we estimate MAAT to be –3 °C. Using the empirical relation between MAAT and summer surface water temperature of Hren and Sheldon (2012), for MAAT of –3 °C we would expect average surface water temperatures (JJA) of ~11 °C. This estimated JJA water temperature is similar to the measured average summer water temperature from our Ngangla Ring Tso record (12.8 °C), and 6 °C cooler than the maximum observed summer water temperature (17 °C). Based on these data we suggest that calculated average (JJA) and maximum (JJA + 6 °C) summer water temperatures reasonably represent the range of warm-season lake water conditions in this region. For Ngangla Ring Tso, this temperature range (11–17 °C) is similar to the tufa sample $T(\Delta_{47})$ values of 10–15 °C (Fig. 7).

The $T(\Delta_{47})$ values for the modern/Holocene gastropod shell samples are similar to the tufa sample temperatures and the estimated warm-season water temperatures at the elevations from which the samples were collected (Fig. 7). Using the approach outlined above and in Figure 6, we estimate MAAT for the modern/Holocene gastropod sample elevations (4550–4880 m) in the range of –2 to –4 °C, average summer surface water temperatures of ~11–12 °C, and maximum water temperatures of ~17–18 °C. The modern/Holocene gastropod shell $T(\Delta_{47})$ values (9–21 °C) are within error of this range, with one exception. A single analysis of sample Zhongba 10-6b, which was collected from a small interdune pond that was isolated from local groundwater, yields a significantly warmer temperature of 31 °C. Based on the general agreement (within 2‰) between the measured $\delta^{18}O$ value of the pond water and the calculated $\delta^{18}O$ value of the water from which the shell grew (Table 3), we have no reason to exclude this sample. However, gastropod temperatures for the three other samples collected from rivers and larger lakes at the same elevation (4570–4580 m: Tsangpo 27, and Zhongba 10-7-2 and 10-10a) agree with each other and are ~10 °C cooler. Thus we suggest that the small, hydrologically isolated interdune pond from which Zhongba 10-6b was collected is not representative of large lake and river water conditions on the plateau. Therefore we do not include the gastropod $T(\Delta_{47})$ value from this location in our modern/Holocene sample average.

The remaining modern/Holocene clumped isotope temperatures cluster in the range of summer average and maximum water temperatures, showing a pronounced warm-season bias. For the modern/Holocene gastropod samples, the average $T(\Delta_{47})$ value is 1 ± 7 °C cooler than (2σ, n = 7; i.e., within uncertainty of) predicted maximum summer water temperatures; if the two tufa samples are included, the clumped

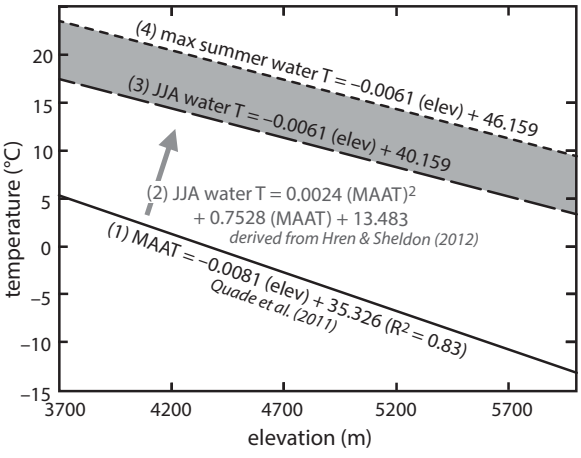

Figure 6. Average temperature versus elevation relations ("lapse rates") used in this study. The solid black line shows the empirically derived relation between mean annual air temperature (MAAT) and elevation of Quade et al. (2011) (equation 1), which is applicable for central and southern Tibet (28–34°N) at elevations of 3700–6000 m. We combined equation 1 with the empirical relation between June-July-August (JJA) water temperature and MAAT of Hren and Sheldon (2012) (equation 2) to derive the summer (JJA) lake surface water temperature versus elevation relation (equation 3, long-dashed line). The calculated JJA water temperature is similar to the average summer temperature observed in the instrumental record from Ngangla Ring Tso (12.8 °C), and 6 °C cooler than the maximum observed summer temperature (17 °C), shown in Figure 4. Based on these data, we suggest that calculated average (JJA) and maximum (JJA + 6 °C) summer water temperatures (equation 4, short-dashed line) reasonably represent warm-season lake water conditions in this region. The gray shaded region corresponds to the gray band in Figure 7.

isotope temperatures for all carbonates average 2 ± 7 °C (2σ, n = 9) cooler than predicted maximum summer water temperatures (Fig. 8). For reference, using the calibration of Henkes et al. (2013) to calculate the gastropod temperatures would result in a modern/Holocene sample average that is ~3 °C cooler than, but also within error of, this estimate. Due to the large scatter, the data do not permit us to distinguish whether the modern/Holocene carbonate temperatures more closely approach average or maximum summer water temperatures. Because modern and Holocene shells collected from nearby locations yield indistinguishable $T(\Delta_{47})$ values, variations in sample age cannot account for the large scatter, which instead might be due to differences in snail habitat (e.g., running or stagnant water) and/or adaptive behavior (e.g., snails migrating to different lake microenvironments). Nevertheless, the warm-season bias is robust.

A warm-season bias in shallow-water tufa samples is not surprising. Huntington et al. (2010) analyzed a small data set of modern lake micrites and tufa from ~300–3300 m elevation in the western United States and found that clumped isotope temperatures generally reflect spring–summer near-surface lake water temperatures. Interestingly, the trend in their data (see Huntington et al., 2010, their fig. 3) suggests that the highest-elevation carbonate temperatures are even more biased toward the warmest lake water temperatures. Our samples were collected >1 km higher than the highest-elevation lake sampled by Huntington et al. (2010), and thus we suggest that tufa $T(\Delta_{47})$ values that are similar to summer average to maximum water temperatures are not surprising.

There is also good reason to expect aquatic gastropod shells to reflect a bias toward shallow-water, warm-season conditions. Previous workers found that the preferred habitat for *Radix* sp. is calm, shallow waters in both lacustrine and riverine environments (Økland, 1990; Glöer, 2002). In winter, individuals either remain active under the ice or migrate to deeper water, with much slower shell growth during this period (see references summarized by Taft et al., 2012). Results from a study of modern Tibetan Plateau *Radix* sp. by Taft et al. (2013) suggest that only ~10%–13% of the shell material grows during the winter months, so that the bulk of the shell growth records a warm-season bias of conditions in the preferred shallow-water habitat of the gastropods. Although a few of the gastropod shells record temperatures nominally in excess of predicted maximum summer water temperatures—which would not be explained by habitat preference and seasonally variable shell growth rates—due to the large analytical uncertainties,

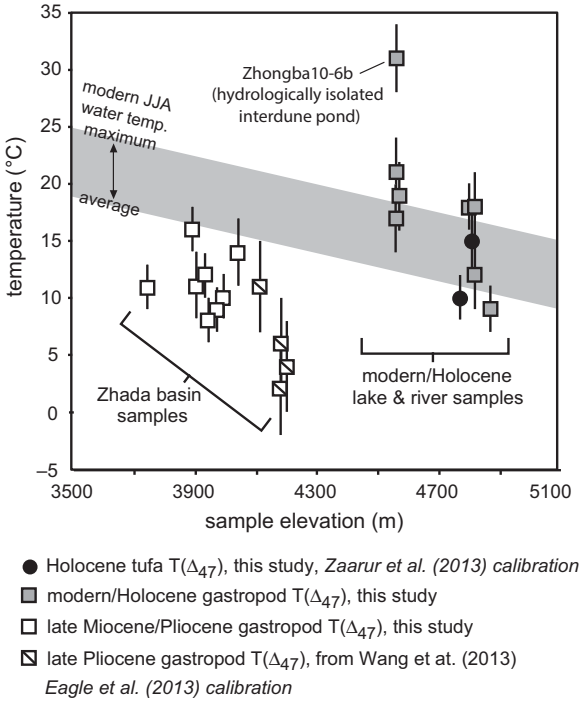

Figure 7. Estimated summer (June-July-August, JJA) lake water temperatures and clumped isotope temperatures [$T(\Delta_{47})$] for lacustrine carbonates from southeastern Tibet. The gray band shows modern warm season (JJA) surface water temperature (JJA average and maximum) as a function of elevation (see text for discussion, and Fig. 6). Holocene tufa sample $T(\Delta_{47})$ values (black circles, error bars indicate one standard error) agree with estimated warm-season water temperatures, but modern/Holocene gastropod shell $T(\Delta_{47})$ values (gray squares) are significantly warmer. Late Miocene–Pliocene gastropod shell $T(\Delta_{47})$ values (open squares, this study; squares with hash mark, Wang et al., 2013) are relatively cooler than $T(\Delta_{47})$ values for modern gastropod samples collected at higher elevations, supporting the hypothesis that the Zhada Basin was cooler at the time the gastropods lived.

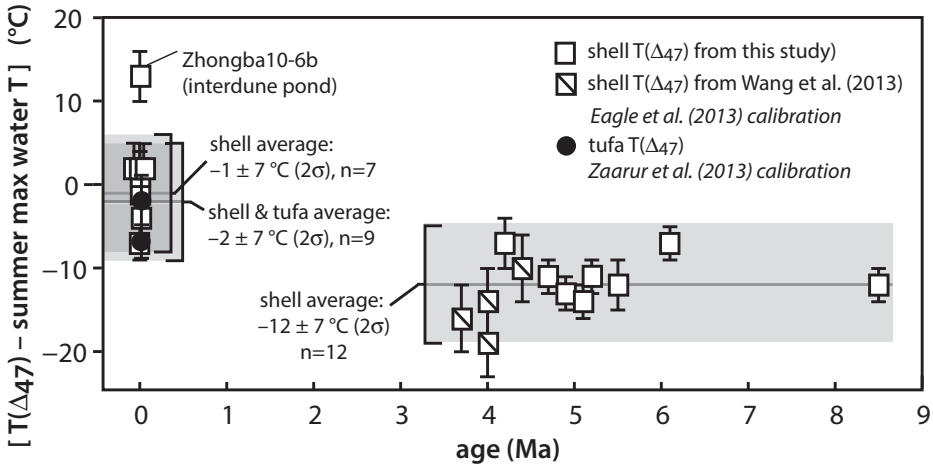

Figure 8. Difference between Zhada Basin clumped isotope temperatures [$T(\Delta_{47})$] and predicted warm-season water temperatures versus sample age. The difference between $T(\Delta_{47})$ for tufa and gastropod shell samples and "summer max T" (the predicted maximum summer water temperature at the modern elevation from which the sample was collected; see text and Fig. 6) is plotted on the *y*-axis, with error bars representing one-standard-error uncertainties in $T(\Delta_{47})$. Gastropod shell sample Zhongba 10-6b is not included in the averages (see text for details). Modern/Holocene sample $T(\Delta_{47})$ values are variable, but the average centers on estimated maximum summer water temperatures. The 3.7–8.5 Ma sample $T(\Delta_{47})$ values are similarly variable, but they are significantly colder than warm-season water temperatures at the modern elevations from which they were collected.

all of the $T(\Delta_{47})$ values agree with estimated summer water temperature within 1 SE.

Modern/Holocene shell and tufa $T(\Delta_{47})$ values are similar to warm-season water temperatures of the environments in which they grew, suggesting that the ancient Zhada Basin snail temperatures can be used to constrain paleoenvironment (and paleoelevation). A word of caution is nonetheless warranted. The sampled fossil taxa from Zhada are the extinct species *Veletinopsis spiralis* and *Radix zandaensis* (Han et al., 2012). The modern aquatic taxa we sampled include *Radix* sp. and other aquatic lymnaeids, and thus we cannot be certain that life cycles and habitat preferences were the same. However, observations by us on modern and ancient environments (Tables 2, 3; Saylor et al., 2009) show that these taxa—modern and extinct—all lived in a shallow-water setting in ponds, and marginal to large lakes and rivers.

New Paleoenvironmental and Paleoelevation Constraints from Zhada Basin $T(\Delta_{47})$ Values

We use the same approach as before to estimate MAAT and representative warm-season lake water temperatures for the modern elevations from which the late Miocene–Pliocene Zhada Basin samples were collected (3750–4210 m; Fig. 7). The equation of Quade et al. (2011) estimates MAAT for the modern Zhada Basin sample elevations to be in the range of 1–5 °C. This range corresponds to average summer surface water temperatures of ~13–17 °C (Hren and Sheldon, 2012), and maximum summer surface water temperatures of ~19–23 °C. These estimates indicate that lake waters at the late Miocene–Pliocene sample elevations are 1–6 °C warmer than lake waters at the modern/Holocene sample elevations, which are ~0.5–1 km higher than the Zhada Basin. The predicted offset depends only on the slope of the water temperature-elevation relations (equations 3 and 4 in Fig. 6) and the elevations from which the samples were collected, and is therefore insensitive to whether the modern/Holocene carbonate temperatures represent average or maximum summer water temperatures. Thus if the Zhada Basin snails lived at their current elevations in a climate regime similar to the modern, we would expect them to record clumped isotope temperatures 1–6 °C warmer than the modern/Holocene samples from higher elevations.

The Zhada Basin data do not follow this prediction (Fig. 7, 8). Instead, the late Miocene–Pliocene shells yield significantly colder temperatures than the modern/Holocene samples. The difference in clumped isotope temperatures (relative to modern summer water temperatures at the elevations from which they were collected) between the modern/Holocene and ancient sample suites is 11 ± 3 °C (2σ, t-test, $p < 2 \times 10^{-6}$, *d.f.* = 19)—suggesting that lake water temperatures were significantly colder in the late Miocene–Pliocene Zhada Basin than the modern. This finding is insensitive to the choice of calibration or to exclusion of subsets of the data. Using the Henkes et al. (2013) calibration for the shell samples instead of the Eagle et al. (2013) calibration, the difference in the population means would be 12 ± 3 °C (2σ). Excluding the tufa data gives the same result as including all the carbonate data (11 ± 3 °C). The Wang et al. (2013) samples analyzed at Johns Hopkins University (Baltimore, Maryland, USA) may not be directly comparable to the samples from this study and from the Eagle et al. (2013) calibration, which were both analyzed at the California Institute of Technology (Pasadena, California,USA). Excluding the Wang et al. (2013) data results in a more conservative but still significant temperature difference between 8.5 and 4.2 Ma and the modern of 9 ± 3 °C (2σ).

The cooler water paleotemperature estimates are broadly consistent with other paleotemperature estimates from secondary carbonate in fossil bone in the Zhada Basin. The $\delta^{18}O$ value of secondary carbonate in bone behaves similarly to soil carbonate (Kohn and Law, 2006; Zanazzi et al., 2007), which generally forms during the warm season (Breecker et al., 2009; Passey et al., 2010; Quade et al., 2011, 2013; Peters et al., 2013; Hough et al., 2014), suggesting that fossil bone–based temperature estimates also should be biased to warm-season soil temperatures (Wang et al., 2013). Soil carbonate clumped isotope data from high elevation (3800–4800 m) Tibetan soils suggest that modern summer soil temperatures in this region exceed MAAT by ~16 °C (Quade et al., 2011). Modern MAAT of 1–5 °C in the Zhada Basin would therefore correspond to warm-season soil temperatures around 17–21 °C—which would be recorded by $\delta^{18}O$ values of secondary carbonate in bone, assuming the temperature of formation is similar to that in soil carbonate. If the 11 ± 3 °C (or 9 ± 3 °C considering only data generated in the Caltech lab) difference suggested by the shell and tufa data similarly impacted soil temperatures, we would expect secondary carbonate in bone to record temperatures around 3–13 °C (5–15 °C). Although the uncertainty in this predicted value is large, the magnitude of temperature change suggested by our data nevertheless is broadly consistent with the lower range of the fossil-based proxy paleotemperature estimate of 15 ± 7 °C for the Zhada Basin ca. 4.2–3.4 Ma (Wang et al., 2013).

Our findings point to late Miocene–Pliocene paleoenvironmental conditions in the Zhada Basin that were significantly cooler than the present, suggesting either that the Miocene–Pliocene climate was cooler than the modern, or that the Zhada Basin was at higher elevations (and hence cooler) in the Miocene–Pliocene. Several data sets suggest that Zhada Basin warming since the Pliocene was not due to climate change. There is substantial evidence for global and regional cooling since 5.3 Ma (Zachos et al., 2001; Thomas et al., 2002) and invariant $T(\Delta_{47})$ values from late Miocene to modern pedogenic carbonates from the Siwaliks of India and Pakistan (Quade et al., 2013). We therefore favor a loss in elevation as the most plausible explanation for the increase in Zhada Basin temperatures.

We estimate the average magnitude of elevation loss experienced by the Zhada sample suite based on the difference between modern/Holocene and late Miocene–Pliocene $T(\Delta_{47})$ values. If the 9 ± 3 °C (2σ, Caltech data only; 11 ± 3 °C including data analyzed at Johns Hopkins) difference between the modern and paleo-$T(\Delta_{47})$ values is due to elevation change, assuming that the modern JJA surface water lapse rate of 6.1 °C/km applies and climate was similar to the modern, it implies 1.5 ± 0.5 km (2σ) of elevation loss (1.8 ± 0.5 km including Johns Hopkins data)—corresponding to an average basin-floor paleoelevation of at least 4.9 km and likely 5.4 km between 8.5 and 4.2 Ma (Fig. 9A). This is a minimum paleoelevation estimate because mid-Pliocene global climate was probably warmer (Dowsett, 2007; Zachos et al., 2001). Similarly, the magnitude of elevation loss experienced by individual snail shell samples can be estimated in the context of the modern/Holocene carbonate and water temperatures and lapse rates (Fig. 9). The uncertainty in estimates from individual samples is large, but the entire gastropod sample suite shows a coherent pattern of higher basin-floor paleoelevation between 8.5 and 3.7 Ma (Fig. 9B), consistent with our 1.5 ± 0.5 km (2σ) average elevation loss estimate.

Our conclusion that the late Miocene–Pliocene Zhada Basin was colder and therefore higher than the present contrasts with previous interpretations of $T(\Delta_{47})$ and pollen data from the region, but is consistent with other paleontological and isotopic data. The difference between our interpretation of snail shell $T(\Delta_{47})$ data and that of Wang et al. (2013) highlights the impact of added context from modern lake water and carbonate temperature data on our results. Conclusions based primarily on palynology suggest that the Miocene Zhada Basin was more temperate than the modern (Li and Li, 1990; Li and Zhou, 2001a, 2001b; Meng et al., 2004; Zhu et al.,

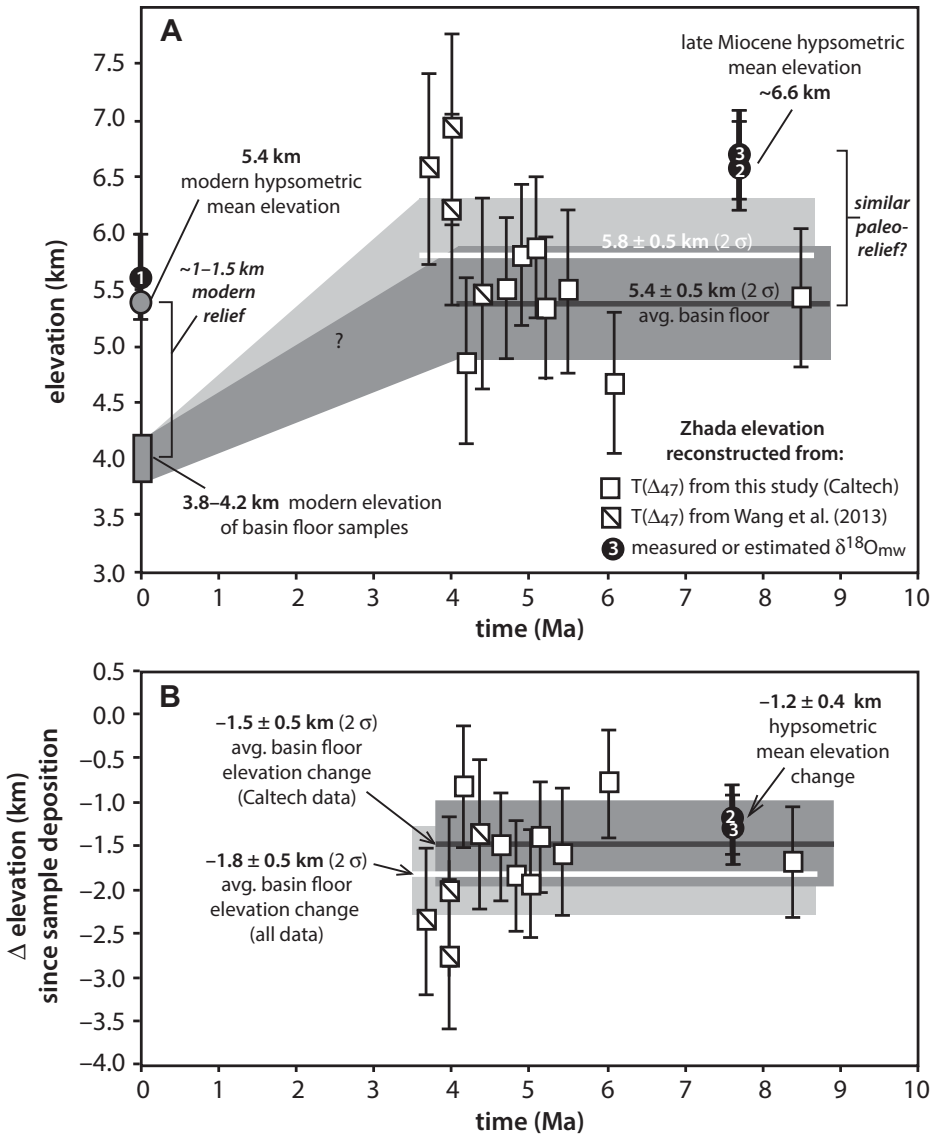

Figure 9. Comparison of paleoelevation estimates and modern basin elevation. Reconstructed basin-floor paleoelevations based on clumped isotope thermometry [$T(\Delta_{47})$] are lower than catchment hypsometric mean (CHM) elevations based on $\delta^{18}O_{mw}$ reconstructions, as expected, and both sets of estimates indicate ~1–1.5 km of elevation loss since the late Miocene. (A) $T(\Delta_{47})$-based paleoelevation estimates for individual samples (squares) assume that (1) the 2 ± 7 °C (2σ) average difference between modern/Holocene carbonate $T(\Delta_{47})$ and maximum summer surface water temperatures (see Fig. 8) applies to the Miocene–Pliocene gastropods, and (2) climate and the modern summer (June-July-August) surface water lapse rate (6.1 °C/km) were the same in the past. Error bars are 2σ and include the uncertainty in each sample's $T(\Delta_{47})$ value and in the temperature offset for the modern/Holocene samples. If mid-Pliocene global climate were warmer, it would make these minimum paleoelevation estimates. The average reconstructed paleoelevation for the sample suite is 5.4 ± 0.5 km based on the 9 ± 3 °C (2σ, California Institute of Technology [Caltech] data only; dark gray bar and line) difference between modern and ancient carbonate temperatures relative to water temperatures at the elevations from which they were collected. Using all data (Caltech and Johns Hopkins University), the temperature difference is 11 ± 3 °C and reconstructed paleoelevation is 5.8 ± 0.5 km (light gray bar and white line). Point 1 shows the estimated hypsometric mean elevation of the modern Zhada catchment (see text). Points 2 and 3 show the reconstructed CHM elevation for sample 0.1SZ53.25B using the clumped isotope temperature of 8 ± 4 °C (point 2) and the temperature of carbonate formation assumed by Saylor et al. (2009) of 7 ± 7 °C (point 3). The difference between basin-floor elevation and CHM elevation (i.e., a proxy for basin relief) reconstructed for the late Miocene is broadly similar to that of the modern Zhada Basin. (B) Results from A plotted as the change in elevation since the time of deposition for each sample. Error bars are 2σ as in A. Black circles show the difference between the $\delta^{18}O_{mw}$-based elevation reconstructions from A and the modern CHM elevation. Estimates of CHM and basin-floor elevation changes are within error, suggesting that the decrease in elevation since the late Miocene–Pliocene was basin wide.

2007). However, the transition from arboreal- to grassland-dominated pollen may be unrelated to the local paleoelevation, and may instead reflect the long-term Neogene history of increasing aridity in the Himalaya and southern Tibet (Clift et al., 2008; Eronen et al., 2009) potentially due to uplift of the northeastern Tibetan Plateau (Tang et al., 2013). Our findings are consistent with the paleontological and isotopic findings of Deng et al. (2011, 2012), which indicate the presence of cold-adapted rhinoceroses and horses living above the tree line in a high-elevation, open habitat in the middle Pliocene.

Revised $\delta^{18}O_{mw}$ Estimates and Isotopic Constraints on Paleoelevation for Southwestern Tibet

We complement the temperature-based paleoelevation estimates with estimates based on a Raleigh distillation model of reconstructed Miocene–Pliocene $\delta^{18}O_{mw}$ values (e.g., Rowley et al., 2001; Rowley, 2007). The isotopic lapse rate in Raleigh distillation models is extremely sensitive to initial low-elevation temperature. Warmer low-elevation temperatures yield lower modeled stable isotope versus elevation lapse rates, resulting in higher reconstructed paleoelevations (Rowley, 2007). There is some evidence for regional cooling and aridification since the Miocene (see Thomas et al., 2002, and references therein). However, we follow the approach of Saylor et al. (2009), assuming no low-elevation temperature change between the Miocene and present (Awashi and Prasad, 1989; Sarkar, 1989; Quade et al., 1995, 2013) and use the modern low-elevation MAAT of 25 °C. This conservative assumption results in minimum reconstructed paleoelevations.

Reconstructed paleoelevation is highly dependent on estimates of $\delta^{18}O_{mw}$, which are

constrained by the $\delta^{18}O$ values of carbonates that precipitated from surface waters (i.e., rivers and lakes). Modern rivers are excellent integrators of the precipitation that falls across the contributing drainage area, especially for large catchments (e.g., Dutton et al., 2005). Gastropods in the Zhada Basin lived in river and lake waters that integrated precipitation in the large paleo-Sutej catchment, so paleo-$\delta^{18}O_{mw}$ values reconstructed from the samples should represent the average elevation at which precipitation feeding those waters fell (hypsometric mean watershed elevations; e.g., Garzione et al., 2000; Rowley et al., 2001; Blisniuk and Stern, 2005; Rowley and Garzione, 2007; Saylor et al., 2009)—subject to modification by evaporation. Evaporation causes ^{18}O enrichment in surface waters, and the $\delta^{18}O$ variability in the ancient record suggests that gastropods from the Zhada Basin, including many of those analyzed in this study, have been influenced by post-precipitation lake evaporation. Reconstructing paleoelevation using an average $\delta^{18}O$ value for the Zhada sample suite likely convolves effects both of elevation and of varying degrees of evaporative enrichment of ancient surface waters. Alternatively, basing Raleigh distillation model reconstructions of paleoelevation on the lowest $\delta^{18}O_{mw}$ estimates from the suite should most closely approximate the $\delta^{18}O$ values of precipitation.

We evaluate the fidelity of this approach by estimating modern elevation based on the lowest modern $\delta^{18}O_{mw}$ value (–17.9‰ VSMOW; Saylor et al., 2009), then estimate Zhada Basin paleoelevation based on $\delta^{18}O_{mw}$ values reconstructed from carbonate $\delta^{18}O$ and $T(\Delta_{47})$ data (Fig. 9A). Using the Raleigh distillation model with initial low-elevation MAAT of 25 °C, the modern $\delta^{18}O_{mw}$ value yields a model elevation of 5.6 ± 0.4 km. This estimate agrees with the mean catchment elevation of 5.4 km extracted from Shuttle Radar Topography Mission digital elevation data for the same water sample, suggesting that this approach should yield useful information about the Miocene hypsometric mean paleoelevation, provided the assumptions discussed above hold and the $\delta^{18}O_{mw}$ value of Miocene precipitation in the Zhada Basin can be estimated.

We estimate the Miocene $\delta^{18}O_{mw}$ value using the Zhada Basin sample with the lowest $\delta^{18}O$ value reported by Saylor et al. (2009)—sample 0.1SZ53.25B (–21.6‰ VPDB, 7.7 Ma), which is assumed to be representative of the least evaporatively ^{18}O-enriched water in which late Miocene gastropods lived. Using this sample $\delta^{18}O$ value and a shell growth temperature of 11 ± 4 °C (2σ) constrained by clumped isotope thermometry [i.e., the $T(\Delta_{47})$ value of the nearest clumped isotope sample, which is also equal to the average $T(\Delta_{47})$ value for all shell samples between 8.5 and 4.4 Ma], yields a $\delta^{18}O_{mw}$ estimate of –22.9‰ VSMOW. The corresponding reconstructed paleoelevation is 6.6 ± 0.4 km, suggesting ~1 km of elevation loss in the Zhada Basin catchment since the late Miocene (Fig. 9B). For this sample, using the 7 ± 7 °C temperature of carbonate formation assumed in the study of Saylor et al. (2009) would result in a $\delta^{18}O_{mw}$ estimate of –23.8‰ VSMOW and an indistinguishable paleoelevation of 6.7 ± 0.4 km.

In principle, using the lowest $\delta^{18}O$ value is appropriate because this avoids the most obvious problem of evaporative enrichment of surface waters, and comparing the lowest modern values and lowest ancient values indicated by our carbonate archives is an internally consistent approach to the problem. In practice, whether the most negative or average $\delta^{18}O$ values (of water or carbonate) are chosen or whether the estimate is considered to be the maximum or average catchment elevation, the answer in terms of elevation change is similar because there is still a decrease in the parameters. The most plausible alternative explanation for the extremely low paleo- $\delta^{18}O$ values is significant climate change since the late Miocene. Specifically, significant low-elevation cooling could produce the observed change in $\delta^{18}O$ values between the late Miocene and modern, but this is at odds with the temperature data from the gastropods.

Comparison of Paleoelevation Estimates and Geodynamic Implications

The difference between the late Miocene–Pliocene basin-floor paleoelevation estimate based on $T(\Delta_{47})$ values (~5.4 km) and the late Miocene catchment average paleoelevation estimate based on reconstructed $\delta^{18}O_{mw}$ values (~6.6 km) is broadly consistent with the relief of the Zhada Basin catchment today (Fig. 9). The temperatures experienced by gastropods living in the Miocene–Pliocene Zhada Basin are a function of the in situ elevation of the basin floor, whereas the $\delta^{18}O_{mw}$ values reflect mean catchment elevations. Thus the difference in paleoelevation estimates based on the two proxies should reflect basin hypsometry and relief. If the late Miocene basin hypsometry were similar to today, we would expect the average basin-floor elevation recorded by the in situ gastropod temperatures to be ~1–1.5 km less than the mean catchment elevation reflected by the $\delta^{18}O_{mw}$ values. Although the uncertainties are large, our estimates using the two methods are offset by approximately this amount, and both suggest similar magnitudes of elevation loss since the late Miocene (Fig. 9B). Thus the data support the notion that the elevation loss was not restricted to the highest-elevation portions of the basin catchment but rather affected the entire basin region.

This loss of elevation across the Zhada Basin catchment is consistent with the models of Murphy et al. (2009) and Saylor et al. (2009), in which elevation loss is driven by arc-parallel (i.e., northwest-southeast) extension accommodated by normal faulting along the Leo Pargil and Gurla Mandhata detachments. However, a broader evaluation of paleoelevation on the Tibetan Plateau is needed to determine whether the loss of elevation observed in the Zhada Basin is a regional phenomenon. If regional elevation loss were observed, it might be explained by the attainment of a limiting elevation and the onset of east-west extension in the Tibetan Plateau (e.g., Molnar and Tapponnier, 1978; Molnar and Lyon-Caen, 1988; Kapp and Guynn, 2004) or ductile escape of material from beneath the plateau (e.g., Clark and Royden, 2001) rather than by local structural control (e.g., Murphy et al., 2009; Saylor et al., 2010).

CONCLUSIONS AND IMPLICATIONS

We analyzed marls and fossil shells from two basins in southern Tibet in order to reconstruct paleoelevations. The effort failed in the Nima Basin because diagenetic alteration of the samples during burial resulted in implausibly high paleotemperatures of up to 61 °C. Clumped isotope temperatures can be diagenetically altered either by mineral dissolution-reprecipitation or by solid-state reordering of ^{13}C-^{18}O bonds if samples are heated above ~100 °C over million-year time scales. The micritic texture, elevated $T(\Delta_{47})$ values, and apparently pristine $\delta^{18}O$ values of the Nima Basin samples can be explained by micro-scale recrystallization in a rock-buffered system. This is consistent with the estimated ~3 km burial depth and temperatures of ~75–90 °C of the samples, because modeling indicates that a doubling of burial depth or geothermal gradient would be required for bond reordering to occur. In the Zhada Basin, much lower $T(\Delta_{47})$ estimates of 8–16 °C were obtained from well-preserved aquatic shells, consistent with primary marginal lake and marsh temperatures.

A key to our Zhada Basin paleoelevation reconstructions is that we were able to contextualize them with sampling of modern and Holocene-age tufa and shells from a range of aquatic environments. Future studies could improve on our own initial "calibration" work with year-round monitoring of water temperature, and focus on specific taxa and their micro-habitat preferences. As the data stand, it

is apparent that tufas and aquatic shells form in warm summer waters with temperatures well in excess of local mean annual temperatures. Modern locations with MAAT at or below 0 °C host tufa and aquatic gastropods recording $T(\Delta_{47})$ values of 9–21 °C, which are similar to measured summertime water temperatures. These comparisons allow us to place interpretations of the $T(\Delta_{47})$ and $\delta^{18}O$ values obtained by previous studies (Saylor et al., 2009; Wang et al., 2013) in a much firmer context.

We confirm that Mio-Pliocene gastropods from the Zhada Basin record Δ_{47} temperatures (average 9 °C from 8.5 to 3.7 Ma; average 11 °C from 8.5 to 4.2 Ma with data from Caltech only) that are much warmer than modern MAAT (1–5 °C). However, these fossil gastropod paleotemperatures are still much cooler than modern/Holocene Δ_{47} temperatures from 0.5- to 1-km-higher elevations, which average 16 °C. We conclude that the Miocene–Pliocene Zhada Basin was cooler than the modern Zhada Basin, consistent with findings of cold-adapted mammal megafauna fossils in the basin. This a very interesting result that cannot be explained by climate changes. If anything, global Mio-Pliocene paleotemperatures were warmer than today, making our paleoelevation estimates probably minima. A 9 ± 3 °C (2σ) average increase in warm-season lake water temperatures indicated by the gastropod Δ_{47} temperatures implies elevation loss of ~1.5 km, corresponding to a reconstructed paleoelevation of 5.4 ± 0.5 km (2σ) for the Mio-Pliocene. Because the gastropods grew in a paleolake, this reconstruction would be for the basin bottom. This estimate can be further compared to estimates based on the $\delta^{18}O$ values of gastropods that grew in the large (ancestral Sutlej or Indus) river that flowed into this paleolake. Waters in the river should reflect the hypsometric mean elevation in the (paleo-)catchment. Our calculations based on these $\delta^{18}O$ values return a very low reconstructed water $\delta^{18}O$ value of –22.9‰ VSMOW, yielding a paleoelevation estimate of 6.6 ± 0.4 km, and suggesting ~1 km of elevation loss. Our study highlights the utility of combining independent paleoelevation estimates based on $T(\Delta_{47})$ and $\delta^{18}O$ values to constrain basin relief through time: this difference between basin floor paleoelevation and hypsometric mean paleoelevation is consistent with the modern difference of ~1–1.5 km, suggesting that the elevation decrease since the Mio-Pliocene was basin wide.

This loss of elevation across the Zhada Basin catchment in the late Neogene probably related to extension along the Leo Pargil and Gurla Mandhata detachments, which may be a local expression of east-west extension across much of the southern Tibetan Plateau at this time.

ACKNOWLEDGMENTS

The authors thank John Eiler for generous laboratory access and support, and David Birlenbach and Nami Kitchen for laboratory assistance. KH acknowledges funding from the National Science Foundation (EAR-1252064 and EAR-1156134) and the donors of the American Chemical Society Petroleum Research Fund (ACS-PRF grant 49709). JQ and AH gratefully acknowledge funding from the COMER Foundation. JS was supported by a grant from the Natural Science Foundation of China (NSFC, 40625008) and the National Science Foundation (EAR-1226984). The authors thank Greg Henkes for sharing the Arrhenius model, Alex Lechler for providing a collegial review of an earlier version of the manuscript, Carmala Garzione and an anonymous reviewer for thorough and helpful formal reviews, and Editor A. Hope Jahren for editorial support.

REFERENCES CITED

Affek, H.P., and Eiler, J.M., 2006, Abundance of mass 47 CO_2 in urban air, car exhaust, and human breath: Geochimica et Cosmochimica Acta, v. 70, p. 1–12, doi:10.1016/j.gca.2005.08.021.

Awashi, N., and Prasad, M., 1989, Siwalik plant fossils from Surai Khola area, western Nepal: Paleobotanist, v. 38, p. 298–318.

Blisniuk, P.M., and Stern, L.A., 2005, Stable isotope paleoaltimetry: A critical review: American Journal of Science, v. 305, p. 1033–1074.

Breecker, D.O., Sharp, Z.D., and McFadden, L.D., 2009, Seasonal bias in the formation and stable isotopic composition of pedogenic carbonate in modem soils from central New Mexico, USA: Geological Society of America Bulletin, v. 121, p. 630–640, doi:10.1130/B26413.1.

Carrapa, B., Huntington, K.W., Clementz, M., Quade, J., Bywater-Reyes, S., Schoenbohm, L.M., and Canavan, R.R., 2014, Uplift of the Central Andes of NW Argentina associated with upper crustal shortening, revealed by multiproxy isotopic analyses: Tectonics, v. 33, doi:10.1002/2013TC003461.

Cassel, E.J., Graham, S.A., and Chamberlain, C.P., 2009, Cenozoic tectonic and topographic evolution of the northern Sierra Nevada, California, through stable isotope paleoaltimetry in volcanic glass: Geology, v. 37, p. 547–550, doi:10.1130/G25572A.1.

Chamberlain, C.P., Mix, H.T., Mulch, A., Hren, M.T., Kent-Corson, M.L., Davis, S.J., Horton, T.W., and Graham, S.A., 2012, The Cenozoic climate and topographic evolution of the western North American Cordillera: American Journal of Science, v. 312, p. 213–262, doi:10.2475/02.2012.05.

Clark, M.K., and Royden, L.H., 2001, Topographic ooze: Building the eastern margin of Tibet by lower crustal flow: Geology, v. 28, p. 703–706.

Clift, P.D., Hodges, K.V., Heslop, D., Hannigan, R., Van Long, H., and Calves, G., 2008, Correlation of Himalayan exhumation rates and Asian monsoon intensity: Nature Geoscience, v. 1, p. 875–880, doi:10.1038/ngeo351.

Csank, A.Z., Tripati, A.K., Patterson, W.P., Eagle, R.A., Rybczynski, N., Ballantyne, A.P., and Eiler, J.M., 2011, Estimates of Arctic land surface temperatures during the early Pliocene from two novel proxies: Earth and Planetary Science Letters, v. 304, p. 291–299, doi:10.1016/j.epsl.2011.02.030.

Cusack, M., England, J., Dalbeck, P., Tudhope, A.W., Fallick, A.E., and Allison, N., 2008, Electron backscatter diffraction (EBSD) as a tool for detection of coral diagenesis: Coral Reefs, v. 27, p. 905–911, doi:10.1007/s00338-008-0414-3.

Cyr, A., Currie, B., and Rowley, D., 2005, Geochemical evaluation of Fenghuoshan Group lacustrine carbonates, north-central Tibet: Implications for the paleoaltimetry of the Eocene Tibetan Plateau: The Journal of Geology, v. 113, p. 517–533, doi:10.1086/431907.

DeCelles, P., Kapp, P., Ding, L., and Gehrels, G., 2007a, Late Cretaceous to middle Tertiary basin evolution in the central Tibetan Plateau: Changing environments in response to tectonic partitioning, aridification, and regional elevation gain: Geological Society of America Bulletin, v. 119, p. 654–680, doi:10.1130/B26074.1.

DeCelles, P., Quade, J., Kapp, P., Fan, M., Dettman, D., and Ding, L., 2007b, High and dry in central Tibet during the Late Oligocene: Earth and Planetary Science Letters, v. 253, p. 389–401, doi:10.1016/j.epsl.2006.11.001.

Deng, T., Wang, X., Fortelius, M., Li, Q., Wang, Y., Tseng, Z.J., Takeuchi, G.T., Saylor, J.E., Säilä, L.K., and Xie, G., 2011, Out of Tibet: Pliocene woolly rhino suggests high-plateau origin of Ice Age megaherbivores: Science, v. 333, p. 1285–1288, doi:10.1126/science.1206594.

Deng, T., Li, Q., Tsang, Z.J., Takeuchi, G.T., Wang, Y., Xie, G., Wang, S., Hou, S., and Wang, X., 2012, Locomotive implication of a Pliocene three-toed horse skeleton from Tibet and its paleo-altimetry significance: Proceedings of the National Academy of Sciences of the United States of America, v. 109, p. 7374–7378, doi:10.1073/pnas.1201052109.

Dennis, K.J., and Schrag, D.P., 2010, Clumped isotope thermometry of carbonatites as an indicator of diagenetic alteration: Geochimica et Cosmochimica Acta, v. 74, p. 4110–4122, doi:10.1016/j.gca.2010.04.005.

Dennis, K.J., Affek, H.P., Passey, B.H., Schrag, D.P., and Eiler, J.M., 2011, Defining an absolute reference frame for 'clumped' isotope studies of CO_2: Geochimica et Cosmochimica Acta, v. 75, p. 7117–7131, doi:10.1016/j.gca.2011.09.025.

Dettman, D.L., Palacios-Fest, M.R., Nkotagu, H.H., and Cohen, A.S., 2005, Paleolimnological investigations of anthropogenic environmental change in Lake Tanganyika: VII. Carbonate isotope geochemistry as a record of riverine runoff: Journal of Paleolimnology, v. 34, p. 93–105, doi:10.1007/s10933-005-2400-x.

Dowsett, H.J., 2007, The PRISM palaeoclimate reconstruction and Pliocene sea-surface temperature, *in* Williams, M., Haywood, A.M., Gregory, J., and Schmidt, D.N., eds., Deep-Time Perspectives on Climate Change: Marrying the Signal from Computer Models and Biological Proxies: London, UK, Micropalaeontological Society (Special Publication), Geological Society of London, p. 459–480.

Dutton, A., Wilkinson, B.H., Welker, J.M., Bowen, G.J., and Lohmann, K.C., 2005, Spatial distribution and seasonal variation in $^{18}O/^{16}O$ of modern precipitation and river water across the conterminous USA: Hydrological Processes, v. 19, p. 4121–4146, doi:10.1002/hyp.5876.

Eagle, R.A., Eiler, J.M., Tripati, A.K., Reis, J.B., Freitas, P.A., Hiebanthanl, C., Wanamaker, A.D., Jr., Taviani, M., Elliot, M., Marenssi, S., Nakamura, K., and Ramirez, P., 2013, The influence of temperature and sea-water carbonate saturation state on ^{13}C-^{18}O bond ordering in bivalve mollusks: Biogeosciences Discussions, v. 10, p. 157–194, doi:10.5194/bgd-10-157-2013.

Eiler, J.M., 2007, "Clumped-isotope" geochemistry: The study of naturally-occurring, multiply-substituted isotopologues: Earth and Planetary Science Letters, v. 262, p. 309–327, doi:10.1016/j.epsl.2007.08.020.

Eiler, J.M., 2011, Paleoclimate reconstruction using carbonate clumped isotope thermometry: Quaternary Science Reviews, v. 30, p. 3575–3588, doi:10.1016/j.quascirev.2011.09.001.

Eiler, J.M., and Schauble, E., 2004, $^{18}O^{13}C^{16}O$ in Earth's atmosphere: Geochimica et Cosmochimica Acta, v. 68, p. 4767–4777, doi:10.1016/j.gca.2004.05.035.

Eronen, J.T., Ataabadia, M.M., Micheelsb, A., Karme, A., Bernor, R.L., and Fortelius, M., 2009, Distribution history and climatic controls of the Late Miocene Pikermian chronofauna: Proceedings of the National Academy of Sciences of the United States of America, v. 106, p. 11,867–11,871, doi:10.1073/pnas.0902598106.

Garzione, C., Quade, J., DeCelles, P., and English, N., 2000, Predicting paleoelevation of Tibet and the Himalaya from delta $\delta^{18}O$ vs. altitude gradients in meteoric water across the Nepal Himalaya: Earth and Planetary Science Letters, v. 183, p. 215–229, doi:10.1016/S0012-821X(00)00252-1.

Garzione, C.N., Hoke, G.D., Libarkin, J.C., Withers, S., MacFadden, B., Eiler, J., Ghosh, P., and Mulch, A.,

2008, Rise of the Andes: Science, v. 320, p. 1304–1307, doi:10.1126/science.1148615.

Garzione, C.N., Auerbach, D.J., Jin-Sook Smith, J., Rosario, J.J., Passey, B.H., Jordan, T.E., and Eiler, J.M., 2014, Clumped isotope evidence for diachronous surface cooling of the Altiplano and pulsed surface uplift of the Central Andes: Earth and Planetary Science Letters, v. 393, p. 173–181, doi:10.1016/j.epsl.2014.02.029.

Ghosh, P., Adkins, J., Affek, H., Balta, B., Guo, W.F., Schauble, E.A., Schrag, D., and Eiler, J.M., 2006a, ^{13}C-^{18}O bonds in carbonate minerals: A new kind of paleothermometer: Geochimica et Cosmochimica Acta, v. 70, p. 1439–1456, doi:10.1016/j.gca.2005.11.014.

Ghosh, P., Garzione, C.N., and Eiler, J.M., 2006b, Rapid uplift of the Altiplano revealed through ^{13}C-^{18}O bonds in paleosol carbonates: Science, v. 311, p. 511–515, doi:10.1126/science.1119365.

Glöer, P., 2002, Die Swassergastropoden Nord- und Mitteleuropas: Hackenheim, Germany, Conchbooks, 327 p.

Guo, W., and Eiler, J.M., 2007, Temperatures of aqueous alteration and evidence for methane generation on the parent bodies of the CM chondrites: Geochimica et Cosmochimica Acta, v. 71, p. 5565–5575, doi:10.1016/j.gca.2007.07.029.

Han, J., Xu, J., He, C., Meng, Q., Zhu, D., Meng, X., Shao, Z., and Yang, C., 2012, The assemblage of gastropod fossils in Zanda basin of Tibet and its biostratigraphy: Acta Geoscience Sinica, v. 33, p. 153–166.

Henkes, G.A., Passey, B.H., Wanamaker, A.D., Grossman, E.L., Ambrose, W.G., and Carroll, M.L., 2013, Carbonate clumped isotope compositions of modern marine mollusk and brachiopod shells: Geochimica et Cosmochimica Acta, v. 106, p. 307–325, doi:10.1016/j.gca.2012.12.020.

Henkes, G.A., Passey, B.H., Grossman, E.L., Shenton, B.J., Pérez-Huerta, A., and Yancey, T.E., 2014, The temperature limits for preservation of primary calcite clumped isotope paleotemperatures: Geochimica et Cosmochimica Acta, v. 139, p. 362–382, doi:10.1016/j.gca.2014.04.040.

Horton, T.W., Sjostrom, D.K., Abruzzese, M.J., Poage, M.A., Waldbauer, J.R., Hren, M., Wooden, J., and Chamberlain, C.P., 2004, Spatial and temporal variation of Cenozoic surface elevation in the Great Basin and Sierra Nevada: American Journal of Science, v. 304, p. 862–888, doi:10.2475/ajs.304.10.862.

Hough, B.G., Fan, M., and Passey, B.H., 2014, Calibration of the clumped isotope geothermometer in soil carbonate in Wyoming and Nebraska, USA: Implications for paleoelevation and paleoclimate reconstruction: Earth and Planetary Science Letters, v. 391, p. 110–120, doi:10.1016/j.epsl.2014.01.008.

Hren, M.T., and Sheldon, N.D., 2012, Temporal variations in lake water temperature: Paleoenvironmental implications of lake carbonate $\delta^{18}O$ and temperature records: Earth and Planetary Science Letters, v. 337, p. 77–84, doi:10.1016/j.epsl.2012.05.019.

Hren, M.T., Sheldon, N.D., Grimes, S.T., Collinson, M.E., Hooker, J.J., Bugler, M., and Lohmann, K.C., 2013, Terrestrial cooling in Northern Europe during the Eocene-Oligocene transition: Proceedings of the National Academy of Sciences of the United States of America, v. 110, p. 7562–7567, doi:10.1073/pnas.1210930110.

Hudson, A.M., and Quade, J., 2013, Long-term east-west asymmetry in monsoon rainfall on the Tibetan Plateau: Geology, v. 41, p. 351–354, doi:10.1130/G33837.1.

Hudson, A.M., Olsen, J.W., and Quade, J., 2014, Radiocarbon dating of interdune wetland deposits to constrain the age of mid- to late Holocene microlithic artifacts from the Zhongba site, southwestern Qinghai-Tibet Plateau: Geoarchaeology, v. 29, p. 33–46, doi:10.1002/gea.21459.

Huntington, K.W., Eiler, J.M., Affek, H.P., Guo, W., Bonifacie, M., Yeung, L.Y., Thiagarajan, N., Passey, B., Tripati, A., Daeron, M., and Came, R., 2009, Methods and limitations of 'clumped' CO_2 isotope (Δ_{47}) analysis by gas-source isotope ratio mass spectrometry: Journal of Mass Spectrometry, v. 44, p. 1318–1329, doi:10.1002/jms.1614.

Huntington, K.W., Wernicke, B.P., and Eiler, J.M., 2010, Influence of climate change and uplift on Colorado Plateau paleotemperatures from carbonate clumped isotope thermometry: Tectonics, v. 29, TC3005, doi:10.1029/2009TC002449.

Huntington, K.W., Budd, D.A., Wernicke, B.P., and Eiler, J.M., 2011, Use of clumped-isotope thermometry to constrain the crystallization temperature of diagenetic calcite: Journal of Sedimentary Research, v. 81, p. 656–669, doi:10.2110/jsr.2011.51.

Kapp, P., and Guynn, J.H., 2004, Indian punch rifts Tibet: Geology, v. 32, p. 993–996, doi:10.1130/G20689.1.

Kapp, P., DeCelles, P.G., Gehrels, G.E., Heizier, M., and Ding, L., 2007, Geological records of the Lhasa-Qiangtang and Indo-Asian collisions in the Nima area of central Tibet: Geological Society of America Bulletin, v. 119, p. 917–933, doi:10.1130/B26033.1.

Kim, S.-T., and O'Neil, J.R., 1997, Equilibrium and nonequilibrium oxygen isotope effects in synthetic carbonates: Geochimica et Cosmochimica Acta, v. 61, p. 3461–3475, doi:10.1016/S0016-7037(97)00169-5.

Kim, S.-T., O'Neil, J.R., Hillaire-Marcel, C., and Mucci, A., 2007, Oxygen isotope fractionation between synthetic aragonite and water: Influence of temperature and Mg^{2+} concentration: Geochimica et Cosmochimica Acta, v. 71, p. 4704–4715, doi:10.1016/j.gca.2007.04.019.

Kempf, O., Blisniuk, P.M., Wang, S., Fang, X., Wrozyna, C., and Schwalb, A., 2009, Sedimentology, sedimentary petrology, and paleoecology of the monsoon-driven, fluviolacustrine Zhada Basin, SW-Tibet: Sedimentary Geology, v. 222, p. 27–41, doi:10.1016/j.sedgeo.2009.07.004.

Kohn, M.J., and Law, J.M., 2006, Stable isotope chemistry of fossil bone as a new paleoclimate indicator: Geochimica et Cosmochimica Acta, v. 70, p. 931–946, doi:10.1016/j.gca.2005.10.023.

Lechler, A.R., Niemi, N.A., Hren, M.T., and Lohmann, K.C., 2013, Paleoelevation estimates for the northern and central proto–Basin and Range from carbonate clumped isotope thermometry: Tectonics, v. 32, p. 295–316, doi:10.1002/tect.20016.

Leier, A., Quade, J., DeCelles, P., and Kapp, P., 2009, Stable isotopic results from paleosol carbonate in South Asia: Paleoenvironmental reconstructions and selective alteration: Earth and Planetary Science Letters, v. 279, p. 242–254, doi:10.1016/j.epsl.2008.12.044.

Leier, A., McQuarrie, N., Garzione, C.N., and Eiler, J., 2013, Oxygen isotope evidence for multiple pulses of rapid surface uplift in the Central Andes, Bolivia: Earth and Planetary Science Letters, v. 371, p. 49–58, doi:10.1016/j.epsl.2013.04.025.

Li, F.L., and Li, D.L., 1990, Latest Miocene Hipparion (Plesiohipparion) of Zanda Basin, *in* Yang, Z.Y., Nie, Z.T., eds., Paleontology of the Ngari Area, Tibet (Xizang): China University Geoscience Press, Wuhan, p. 186–193.

Li, J., and Zhou, Y., 2001a, Palaeovegetation type analysis of the late Pliocene in Zanda basin of Tibet: Journal of Palaeogeography, v. 14, p. 52–58.

Li, J., and Zhou, Y., 2001b, Pliocene palynoflora from the Zanda Basin west Xizang (Tibet), and the palaeoenvironment: Acta Micropalaeontologica Sinica, v. 18, p. 89–96.

Meng, X., Zhu, D., Shao, Z., Yang, C., Sun, L., Wang, J., Han, T., Du, J., Han, J., and Yu, J., 2004, Discovery of rhinoceros fossils in the Pliocene in the Zanda basin, Ngari, Tibet: Geological Bulletin of China, v. 23, p. 609–612.

Meng, X.G., Zhu, D.G., Shao, Z.G., Yang, C.B., Han, J.N., Yu, J., Meng, Q.W., and Lu, R.P., 2008, Late Cenozoic stratigraphy and paleomagnetic chronology of the Zanda basin, Tibet, and records of the uplift of the Qinghai-Tibet Plateau: Acta Geologica Sinica (English edition), v. 82, p. 63–72.

Molnar, P., and Lyon-Caen, H., 1988, Some simple physical aspects of the support, structure, and evolution of mountain belts, *in* Clark, S.P., Jr., Burchfiel, B.C., and Suppe, J., eds., Processes in Continental Lithospheric Deformation: Geological Society of America Special Paper 218, p. 179–207, doi:10.1130/SPE218-p179.

Molnar, P., and Stock, J.M., 2009, Slowing of India's convergence with Eurasia since 20 Ma and its implications for Tibetan mantle dynamics: Tectonics, v. 28, TC3001, doi:10.1029/2008TC002271.

Molnar, P., and Tapponnier, P., 1978, Active tectonics of Tibet: Journal of Geophysical Research, v. 83, p. 5361–5375, doi:10.1029/JB083iB11p05361.

Mulch, A., Sarna-Wojcicki, A.M., Perkins, M.E., and Chamberlain, C.P., 2008, A Miocene to Pleistocene climate and elevation record of the Sierra Nevada (California): Proceedings of the National Academy of Sciences of the United States of America, v. 105, p. 6819–6824, doi:10.1073/pnas.0708811105.

Murphy, M., Saylor, J., and Ding, L., 2009, Late Miocene topographic inversion in southwest Tibet based on integrated paleoelevation reconstructions and structural history: Earth and Planetary Science Letters, v. 282, p. 1–9, doi:10.1016/j.epsl.2009.01.006.

Økland, J., 1990, Lakes and Snails: Environment and Gastropoda in 1,500 Norwegian Lakes, Ponds and Rivers: Oegstgeest, Universal Book Services–Dr. W. Backhuys, 515 p.

Passey, B.H., and Henkes, G.A., 2012, Carbonate clumped isotope bond reordering and geospeedometry: Earth and Planetary Science Letters, v. 351, p. 223–236, doi:10.1016/j.epsl.2012.07.021.

Passey, B.H., Levin, N.E., Cerling, T.E., Brown, F.H., and Eiler, J.M., 2010, High-temperature environments of human evolution in East Africa based on bond ordering in paleosol carbonates: Proceedings of the National Academy of Sciences of the United States of America, v. 107, p. 11,245–11,249, doi:10.1073/pnas.1001824107.

Pérez-Huerta, A., Grossman, E.L., Henkes, G.A., Passey, B.H., and Shenton, B., 2014, Electron backscatter diffraction (EBSD) as a tool for evaluating fossil preservation for carbonate clumped isotope paleothermometry: Mineralogical Magazine, Goldschmidt abstract (in press).

Peters, N.A., Huntington, K.W., and Hoke, G.D., 2013, Hot or not? Impact of seasonally variable soil carbonate formation on paleotemperature and O-isotope records from clumped isotope thermometry: Earth and Planetary Science Letters, v. 361, p. 208–218, doi:10.1016/j.epsl.2012.10.024.

Polissar, P.J., Freeman, K.H., Rowley, D.B., McInerney, F.A., and Currie, B.S., 2009, Paleoaltimetry of the Tibetan Plateau from D/H ratios of lipid biomarkers: Earth and Planetary Science Letters, v. 287, p. 64–76, doi:10.1016/j.epsl.2009.07.037.

Quade, J., Cater, J., Ojha, T., Adam, J., and Harrison, T., 1995, Late Miocene environmental change in Nepal and the northern Indian subcontinent: Stable isotopic evidence from paleosols: Geological Society of America Bulletin, v. 107, p. 1381–1397, doi:10.1130/0016-7606(1995)107<1381:LMECIN>2.3.CO;2.

Quade, J., Garzione, C., and Eiler, J., 2007, Paleosol carbonate in paleoelevation reconstruction, *in* Kohn, M., ed., Paleoelevation: Geochemical and Thermodynamic Approaches: Reviews in Mineralogy and Geochemistry: Mineralogical Society of America Bulletin, v. 66, p. 53–87.

Quade, J., Breecker, D.O., Daeron, M., and Eiler, J., 2011, The paleoaltimetry of Tibet: An isotopic perspective: American Journal of Science, v. 311, p. 77–115, doi:10.2475/02.2011.01.

Quade, J., Eiler, J., Daëron, M., and Achyuthan, H., 2013, The clumped isotope geothermometer in soil and paleosol carbonate: Geochimica et Cosmochimica Acta, v. 105, p. 92–107, doi:10.1016/j.gca.2012.11.031.

Rowley, D.B., 2007, Stable isotope–based paleoaltimetry: Theory and validation, *in* Kohn, M.J., ed., Paleoaltimetry: Geochemical and Thermodynamic Approaches: Reviews in Mineralogy and Geochemistry 66, p. 23–52.

Rowley, D., and Currie, B., 2006, Palaeo-altimetry of the late Eocene to Miocene Lunpola basin, central Tibet: Nature, v. 439, p. 677–681, doi:10.1038/nature04506.

Rowley, D.B., and Garzione, C.N., 2007, Stable isotope-based paleoaltimetry: Annual Reviews in Earth and Planetary Science, v. 35, p. 463–508.

Rowley, D., Pierrehumbert, R., and Currie, B., 2001, A new approach to stable isotope–based paleoaltimetry: Implications for paleoaltimetry and paleohypsometry of the High Himalaya since the Late Miocene: Earth and Planetary Science Letters, v. 188, p. 253–268, doi:10.1016/S0012-821X(01)00324-7.

Sarkar, S., 1989, Siwalik pollen succession from Surai Khola of western Nepal and its reflection on paleoecology: Paleobotanist, v. 38, p. 319–324.

Saylor, J.E., 2008, The late Miocene through modern evolution of the Zhada basin, south-western Tibet [Ph.D. thesis]: Tucson, University of Arizona, Department of Geosciences, p. 306.

Saylor, J.E., Quade, J., Dettman, D.L., DeCelles, P.G., Kapp, P.A., and Ding, L., 2009, The late Miocene through present paleoelevation history of southwestern Tibet: American Journal of Science, v. 309, p. 1–42, doi:10.2475/01.2009.01.

Saylor, J.E., DeCelles, P.G., and Quade, J., 2010, Climate-driven environmental change in the Zhada basin, southwestern Tibetan Plateau: Geosphere, v. 6, p. 74–92, doi:10.1130/GES00507.1.

Schauble, E.A., Ghosh, P., and Eiler, J.M., 2006, Preferential formation of ^{13}C-^{18}O bonds in carbonate minerals, estimated using first-principles lattice dynamics: Geochimica et Cosmochimica Acta, v. 70, p. 2510–2529, doi:10.1016/j.gca.2006.02.011.

Schmid, T.W., and Bernasconi, S.M., 2010, An automated method for 'clumped-isotope' measurements on small carbonate samples: Rapid Communications in Mass Spectrometry, v. 24, p. 1955–1963, doi:10.1002/rcm.4598.

Snell, K.E., Thrasher, B.L., Eiler, J.M., Koch, P.L., Sloan, L.C., and Tabor, N.J., 2013, Hot summers in the Bighorn Basin during the early Paleogene: Geology, v. 41, p. 55–58, doi:10.1130/G33567.1.

Taft, L., Wiechert, U., Riedel, F., Weynell, M., and Zhang, H.C., 2012, Sub-seasonal oxygen and carbon isotope variations in shells of modern *Radix* sp. (Gastropoda) from the Tibetan Plateau: Potential of a new archive for palaeoclimatic studies: Quaternary Science Reviews, v. 34, p. 44–56, doi:10.1016/j.quascirev.2011.12.006.

Taft, L., Wiechert, U., Zhang, H.C., Lei, G.L., Mischke, S., Plessen, B., Weynell, M., Winkler, A., and Riedel, F., 2013, Oxygen and carbon isotope patterns archived in shells of the aquatic gastropod *Radix*: Hydrologic and climatic signals across the Tibetan Plateau in sub-monthly resolution: Quaternary International, v. 290, p. 282–298, doi:10.1016/j.quaint.2012.10.031.

Tang, H., Micheels, A., Eronen, J.T., Ahrens, B., and Fortelius, M., 2013, Asynchronous responses of East Asian and Indian summer monsoons to mountain uplift shown by regional climate modelling experiments: Climate Dynamics, v. 40, p. 1531–1549, doi:10.1007/s00382-012-1603-x.

Thomas, J.V., Parkash, B., and Mohindra, R., 2002, Lithofacies and palaeosol analysis of the Middle and Upper Siwalik Groups (Plio-Pleistocene), Haripur-Kolar section, Himachal Pradesh, India: Sedimentary Geology, v. 150, p. 343–366, doi:10.1016/S0037-0738(01)00203-2.

Wang, S.F., Zhang, W.L., Fang, X.M., Dai, S., and Kempf, O., 2008, Magnetostratigraphy of the Zanda basin in southwest Tibet Plateau and its tectonic implications: Chinese Science Bulletin, v. 53, p. 1393–1400, doi:10.1007/s11434-008-0132-9.

Wang, Y., Deng, T., Biasatti, D., 2006, Ancient diets indicate significant uplift of southern Tibet after ca. 7 Ma: Geology, v. 34, p. 309–312, doi:10.1130/G22254.1.

Wang, Y., Xu, Y.F., Khawaja, S., Passey, B.H., Zhang, C., Wang, X., Qiang, L., Tseng, Z.J., Takeuchi, G.T., Deng, T., and Xie, G.P., 2013, Diet and environment of a mid-Pliocene fauna from southwestern Himalaya: Paleo-elevation implications: Earth and Planetary Science Letters, v. 376, p. 43–53, doi:10.1016/j.epsl.2013.06.014.

Zaarur, S., Olack, G., and Affek, H.P., 2011, Paleo-environmental implication of clumped isotopes in land snail shells: Geochimica et Cosmochimica Acta, v. 75, p. 6859–6869, doi:10.1016/j.gca.2011.08.044.

Zaarur, S., Affek, H.P., Brandon, M.T., 2013, A revised calibration of the clumped isotope thermometer: Earth and Planetary Science Letters, v. 382, p. 47–57.

Zachos, J., Pagani, M., Sloan, L., Thomas, E., and Billups, K., 2001, Trends, rhythms, and aberrations in global climate 65 Ma to present: Science, v. 292, p. 686–693, doi:10.1126/science.1059412.

Zanazzi, A., Kohn, M.J., MacFadden, B.J., and Terry, D.O., 2007, Large temperature drop across the Eocene-Oligocene transition in central North America: Nature, v. 445, p. 639–642.

Zhang, Q., Wang, F., Ji, H., and Huang, W., 1981, Pliocene sediments of the Zanda basin, Tibet: Journal of Stratigraphy, v. 5, p. 216–220.

Zhu, D., Meng, X., Shoa, Z., Yang, C., Han, J., Yu, J., Meng, Q., and Lu, R., 2007, Evolution of the paleovegetation, paleoenvironment and paleoclimate during Pliocene–early Pleistocene in Zhada Basin, Ali, Tibet: Acta Geologica Sinica, v. 81, p. 295–306.

Science Editor: A. Hope Jahren
Associate Editor: Troy Rasbury

Manuscript Received 20 September 2013
Revised Manuscript Received 4 June 2014
Manuscript Accepted 2 July 2014

Printed in the USA